Molecular Microbiology (2014) 92(2), 338–355 ■
doi:10.1111/mmi.12561
First published online 17 March 2014

Biotrophy-specific downregulation of siderophore biosynthesis in *Colletotrichum graminicola* is required for modulation of immune responses of maize

Emad Albarouki,[1,2] Lukas Schafferer,[3] Fanghua Ye,[1,4] Nicolaus von Wirén,[1,4] Hubertus Haas[3] and Holger B. Deising[1,2]*

[1]*Martin-Luther-Universität Halle-Wittenberg, Interdisziplinäres Zentrum für Nutzpflanzenforschung (IZN), Betty-Heimann-Str. 3, D-06120 Halle (Saale), Germany.*

[2]*Martin-Luther-Universität Halle-Wittenberg, Institut für Agrar- und Ernährungswissenschaften, Phytopathologie und Pflanzenschutz, Betty-Heimann-Str. 3, D-06120 Halle (Saale), Germany.*

[3]*Medizinische Universität Innsbruck, Sektion für Molekularbiologie/Biozentrum, Innrain 80/82, A-6020 Innsbruck, Austria.*

[4]*Leibniz-Institut für Pflanzengenetik und Kulturpflanzenforschung (IPK), Corrensstr. 3, Molekulare Pflanzenernährung, D-06466 Seeland – Gatersleben, Germany.*

Summary

The hemibiotrophic maize pathogen *Colletotrichum graminicola* synthesizes one intracellular and three secreted siderophores. *eGFP* fusions with the key siderophore biosynthesis gene, *SID1*, encoding L-ornithine-N^5-monooxygenase, suggested that siderophore biosynthesis is rigorously downregulated specifically during biotrophic development. In order to investigate the role of siderophores during vegetative development and pathogenesis, *SID1*, which is required for synthesis of all siderophores, and the non-ribosomal peptide synthetase gene *NPS6*, synthesizing secreted siderophores, were deleted. Mutant analyses revealed that siderophores are required for vegetative growth under iron-limiting conditions, conidiation, ROS tolerance, and cell wall integrity. Δ*sid1* and Δ*nps6* mutants were hampered in formation of melanized appressoria and impaired in virulence. In agreement with biotrophy-specific downregulation of siderophore biosynthesis, Δ*sid1* and Δ*nps6* strains were not affected in biotrophic development, but spread of necrotrophic hyphae was reduced. To address the question why siderophore biosynthesis is specifically downregulated in biotrophic hyphae, maize leaves were infiltrated with siderophores. Siderophore infiltration alone did not induce defence responses, but formation of biotrophic hyphae in siderophore-infiltrated leaves caused dramatically increased ROS formation and transcriptional activation of genes encoding defence-related peroxidases and PR proteins. These data suggest that fungal siderophores modulate the plant immune system.

Accepted 18 February, 2014. *For correspondence. E-mail holger.deising@landw.uni-halle.de; Tel. (+49) 345 5522660; Fax (+49) 345 5522120.

Introduction

Iron is an essential nutrient and the major redox element in all eukaryotes. Paradoxically, although iron is one of the most abundant elements on Earth, its bioavailability is extremely low. At neutral pH, the solubility product of $Fe^{(III)}$, the main oxidation state in an aerobic environment, is less than 10^{-18} M (Neilands *et al.*, 1987). As compared to iron-rich terrestrial environments, the availability of iron may even be significantly lower for pathogenic fungi, as free iron does basically not exist in mammalian and plant hosts (Weinberg, 1978; 2009; Expert, 1999), due to tight sequestration by ferritin, transferrins and/or several other iron-binding proteins (Ratledge and Dover, 2000; Arosio and Levi, 2002). As a consequence, pathogenic fungi have evolved two high-affinity iron acquisition strategies allowing them to compete with their hosts for iron, by either siderophore-mediated or reductive iron acquisition (Philpott, 2006; Haas *et al.*, 2008).

All siderophores identified in pathogenic asco- and basidiomycetes so far belong to the hydroxamate type of siderophores (Haas *et al.*, 2008). The first step in the biosynthesis of hydroxamate siderophores in fungi is N^5-hydroxylation of L-ornithine, catalysed by the key enzyme of this pathway, L-ornithine-N^5-monooxygenase (Haas *et al.*, 2008; Fig. S1). Deletion of the corresponding gene, *SID1*, blocks synthesis of all intracellular and secreted siderophores. The *Aspergillus nidulans* mutant deficient in the *SID1* homologue *sidA* exhibits severe

growth defects, due to the lack of reductive iron assimilation (Eisendle *et al*., 2003). Closely related pathogenic *Aspergillus* species, i.e. the plant pathogen *A. oryzae* and the mammalian pathogen *A. fumigatus*, are able to utilize reductive iron assimilation, which compensates for the loss of siderophores. Therefore, the lack of siderophore biosynthesis affects vegetative growth under iron-limiting conditions of these pathogenic species only to some extent (Haas *et al*., 2008).

In subsequent steps of siderophore biosynthesis, the hydroxamate group is formed by N^5-acylation of N^5-hydroxyornithine, and siderophore synthesis is completed by covalently linking the hydroxamate residues by non-ribosomal peptide synthetases (NRPSs). NRPSs are large multifunctional enzymes with modular structure that synthesize peptides in a ribosome-independent manner (Mootz *et al*., 2002). These enzymes, which are exclusively found in bacteria and fungi, require activation by 4′-phosphopantetheinylation (Horbach *et al*., 2009; Marquez-Fernandez *et al*., 2007; Wiemann *et al*., 2012; Fig. S1). Only one of the NRPSs, i.e. Nps6, is required for synthesis of secreted siderophores. In *A. fumigatus* and in several necrotrophic plant pathogens, i.e. the Southern Corn Leaf Blight fungus *Cochliobolus heterostrophus*; the causal agent of brown spot disease in rice, *Cochliobolus miyabeanus*; the causal agent of head blight of wheat and barley and ear rot of maize, *Fusarium graminearum*; and the causal agent of black spot disease on virtually all economically important *Brassica* species, *Alternaria brassicicola*, inactivation of *NPS6* homologues affected rates of vegetative growth, asexual sporulation, and/or oxidative stress tolerance under iron-limiting conditions (Oide *et al*., 2006; Schrettl *et al*., 2007). Intracellular siderophores are synthesized by Nps2 (Haas *et al*., 2008).

Competitive iron acquisition is indispensable for hyphal growth in iron-limited environments and can therefore be regarded as a pathogenicity factor in both mammalian and plant hosts. Deletion of the L-ornithine-N^5-monooxygenase gene *sid*A of the mammalian pathogen *A. fumigatus* abrogated siderophore biosynthesis and prevented the establishment of pulmonary aspergillosis in a mouse model (Schrettl *et al*., 2004; Hissen *et al*., 2005). In contrast, inactivation of reductive iron assimilation in this fungus had no effect on virulence (Schrettl *et al*., 2004). Likewise, in the above mentioned necrotrophs *F. graminearum*, *C. heterostrophus*, *C. miyabeanus* and *A. brassicicola*, siderophore-mediated iron uptake plays the predominant role in virulence (Oide *et al*., 2006; Park *et al*., 2006; Greenshields *et al*., 2007). *NPS2* deletion experiments in the rice blast fungus *Magnaporthe oryzae* suggested that the intracellular siderophore ferricrocin may also be involved in virulence (Hof *et al*., 2007).

By contrast, in the biotrophic plant pathogenic smut fungi *Microbotryum violaceum*, infecting white campion (*Silene latifolia*), and *Ustilago maydis*, infecting maize (*Zea mays*), reductive iron assimilation, but not siderophore-mediated iron uptake, is required for full virulence (Mei *et al*., 1993; Birch and Ruddat, 2005). Supporting the idea that reductive iron assimilation is required for virulence of biotrophs, Albarouki and Deising (2013) have shown that the ferroxidase gene *FET3-1* of the hemibiotroph *Colletotrichum graminicola* is specifically expressed in and required for development of biotrophic hyphae, and that this gene is a determinant of virulence.

Hemibiotrophic plant pathogens like *C. graminicola* are ideally suited to analyse the role of the two fungal high-affinity iron acquisition strategies, mediated via either siderophores or reductive iron assimilation, in the same genetic background during pathogenesis. As a first step in the infection process, the maize leaf anthracnose and stem rot fungus *C. graminicola* differentiates a dome-shaped infection cell, called an appressorium, on the epidermis of the leaf. The invading infection vesicle and primary hyphae invaginate the plasma membrane of the host and re-programme the host cell, resulting in prevention of host cell death and re-direction of nutrients to the infection site (Behr *et al*., 2010). During this biotrophic stage of pathogenesis, the hyphae are tightly surrounded by the plasma membrane of the plant, and the bifacial matrix surrounding the hyphae is likely extremely poor in nutrients, including iron. Upon perception of a hitherto unidentified signal, the pathogen changes its lifestyle and differentiates thin, fast growing, highly destructive necrotrophic hyphae (Bergstrom and Nicholson, 1999; Horbach *et al*., 2011; Horbach and Deising, 2013). However, whether employment of the two high-affinity iron acquisition strategies is functionally linked to the development of biotrophic and necrotrophic infection structures, and whether differential utilization of these strategies is required to establish a hemibiotrophic lifestyle and a compatible parasitic interaction is unknown.

Using *SID1*:*eGFP* fusions and live-cell imaging, we show specific expression of *SID1* in secondary hyphae, indicating that siderophore-mediated iron acquisition is employed during necrotrophy, and rigorously downregulated in biotrophic hyphae. Targeted deletion of *SID1* and *NPS6* demonstrated that siderophore biosynthesis is required for efficient spreading of necrotrophic hyphae and full virulence of *C. graminicola*. Furthermore, diaminobenzidine staining and qRT-PCR showed that leaves infiltrated with the siderophore coprogen activated broad spectrum defence responses when biotrophic hyphae invaded epidermal cells. Siderophore infiltration without subsequent inoculation did not evoke defence responses.

These data suggest that secretion of siderophores during infection by biotrophs modulates the plant immune system.

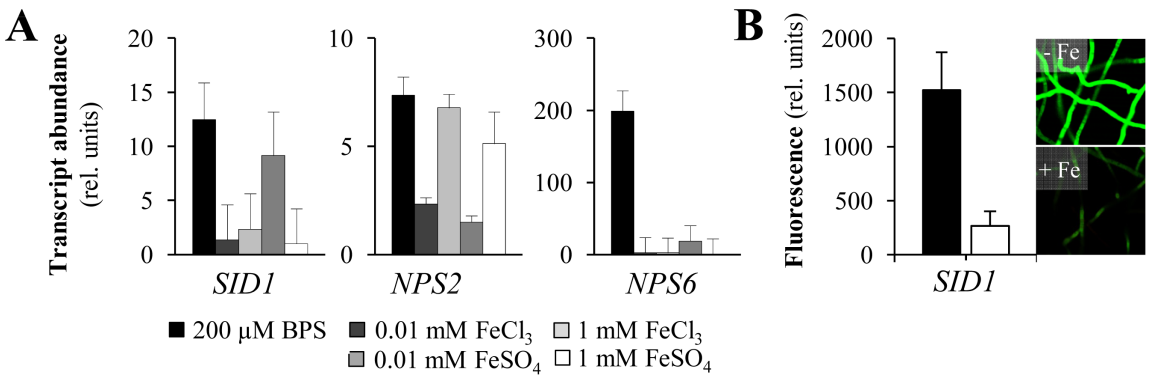

Fig. 1. Iron availability regulates transcript abundance of *SID1*, *NPS2* and *NPS6*.
A. Relative transcript abundance of the siderophore synthesis genes *SID1, NPS2* and *NPS6* at different iron supplies. Actin *ACT1* and histone *H3* transcripts were used as references.
B. Control of *SID1* expression by the availability of iron, as measured by the eGFP-fluorescence of the WT strain harbouring the P_{SID1}:*eGFP* fusion. Fluorescence intensity is given in relative units.

Results

The availability of iron controls expression of the siderophore biosynthesis genes SID1, NPS2 and NPS6

Genome mining of pathogenic Pezizomycotina, Taphrinomycotina and some Basidiomycota suggested that remarkable differences in fungal iron acquisition exist, possibly depending on their lifestyle. Most filamentous Ascomycota, e.g. several *Aspergillus*, *Fusarium* and *Mycosphaerella* species, harbour only a single copy of the key gene of siderophore synthesis, *SID1*, and thus, a single L-ornithine-N^5-monooxygenase (Fig. S2A; Sid1). This also holds true for the maize anthracnose fungus *C. graminicola*. The biotrophic maize pathogen and basidiomycete *U. maydis* harbours a *SID1* gene, but utilizes reductive iron assimilation during pathogenesis (Eichhorn *et al.*, 2006). The rust fungus *Puccinia graminis*, also a biotroph, has a *SID1*-related gene, but the identity of the derived protein with that of *SID1* of *C. graminicola* is only 25%, so that functional assays would be required to confirm that the rust protein indeed exhibits L-ornithine-N^5-monooxygenase activity. Interestingly, the genome of the biotrophic powdery mildew fungus *B. graminis* f. sp. *hordei* does not contain a *SID1* homologue.

In contrast to Sid1 proteins, a multitude of NRPSs exists in fungal species, as derived from the genomes inspected. In *C. graminicola*, nine NRPS proteins, and at least seven NRPS/PKS hybrids exist. Nps6 proteins are highly conserved among the Euascomycota, including plant and human pathogens (Fig. S2B). Functional analysis of all non-ribosomal peptide synthetases in *C. heterostrophus* revealed that only Nps6, the enzyme required to synthesize secreted siderophores, is involved in virulence and resistance to oxidative stress (Lee *et al.*, 2005; Oide *et al.*, 2006). Only a single copy of *NPS6* exists in the genome of *C. graminicola* (Fig. S2B).

The availability of iron controls transcript abundance of the siderophore synthesis genes *SID1*, *NPS2* and *NPS6*. Under iron-limiting conditions, as induced by addition of 200 µM of the iron scavenger bathophenanthroline disulphonate (BPS), enhanced levels of *SID1*, *NPS2* and *NPS6* transcripts were found in vegetative hyphae. $Fe^{(III)}$, which is taken up by siderophores, efficiently down-regulated *SID1* and *NPS6* transcripts at concentrations corresponding to 10 µM or 1 mM. Interestingly, high iron concentrations led to increased transcript levels of *NPS2* required for synthesis of intracellular storage siderophores and control of intracellular iron homeostasis. Similar transcriptional responses were observed after application of $Fe^{(II)}$, although adjusting the $Fe^{(II)}$ concentration to 10 µM reduced *SID1* transcript abundance only slightly (Fig. 1A). To use an independent method showing that iron availability regulates siderophore biosynthesis, a *C. graminicola* strain harbouring an *eGFP* gene fused to the *SID1* promoter was constructed (Fig. S3), and eGFP fluorescence of vegetative hyphae was used as a measure of *SID1* promoter activity. As expected, in the presence of 200 µM BPS strong eGFP fluorescence was found, while in the presence of 1 mM $FeSO_4$ eGFP fluorescence decreased dramatically (Fig. 1B).

SID1 and NPS6 are required for vegetative growth under iron-limiting conditions, tolerance to ROS, and conidiation

In order to functionally characterize siderophore biosynthesis, we deleted the ornithine-N^5-monooxygenase gene *SID1*, required for synthesis of all hydroxamate siderophores, as well as the non-ribosomal peptide synthetase gene *NPS6*, specifically required for synthesis of all secreted siderophores (Fig. S4). The growth defect under iron-limiting conditions, as well as the defects in infection

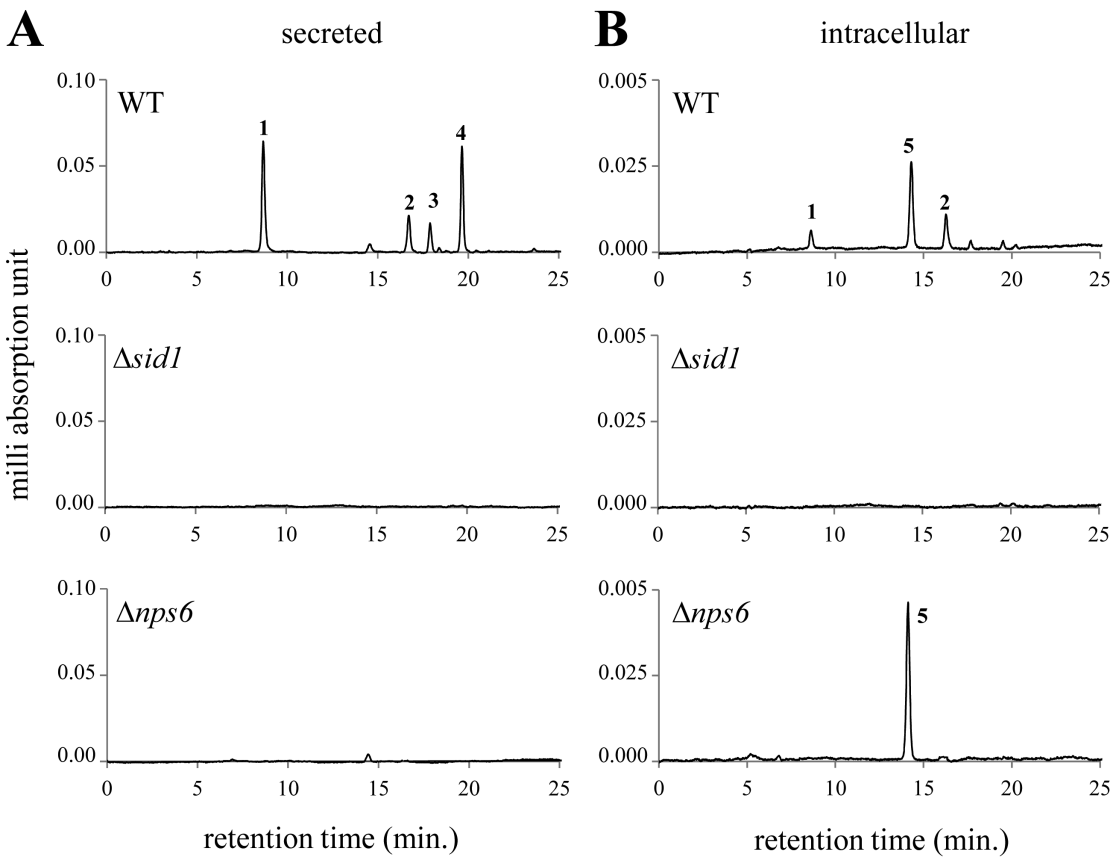

Fig. 2. HPLC-MS analysis of secreted and intracellular siderophores of *C. graminicola* strains.
A. Secreted siderophores analysed in culture media of the WT, Δ*sid1* and Δ*nps6*, strains. Δ*sid1* and Δ*nps6* are unable to produce any extracellular siderophores produced by the wild-type strain (WT).
B. Intracellular siderophore isolated from vegetative fungal mycelia. WT and Δ*nps6*, but not Δ*sid1* strains are able to produce the intracellular siderophore ferricrocin.
Peak 1, dimerumic acid; peak 2, coprogen B; peak 3, N^{α}-methylcoprogen B; peak 4, coprogen; peak 5, ferricrocin.

structure differentiation and virulence were fully complemented by transforming the Δ*sid1* deletion strain with a *SID1*:*eGFP* construct. Furthermore, all independent deletion strains tested showed identical phenotypes, collectively indicating that the phenotype of the Δ*sid1* deletion strain was indeed caused by the deletion of *SID1*. Genetic complementation of Δ*nps6* mutants was not successful, due to the large size of the *NPS6* gene. However the mutant phenotype was rescued by chemical complementation (see below), suggesting that the phenotype of all independent Δ*nps6* strains was indeed due to the deletion of *NPS6*. The WT strain CgM2 and the resulting Δ*sid1* and Δ*nps6* mutants of *C. graminicola* were grown in Sundström minimal medium inducing siderophore biosynthesis (Sundström, 1964), and the culture filtrates as well as the cell homogenates were used to analyse secreted and intracellular siderophores. HPLC (Fig. 2), in combination with mass spectrometry analyses (Fig. S5), revealed that *C. graminicola* produces three secreted siderophores, i.e. coprogen, coprogen B, and methyl-coprogen B, as well as the intracellular storage siderophore ferricrocin, confirming and extending previous data (Horbach *et al.*, 2009). In addition, dimerumic acid was identified, representing either a siderophore precursor or a degradation product (Fig. 2 and Fig. S5). As expected, Δ*sid1* mutants were not able to synthesize any siderophore, whereas Δ*nps6* mutants were specifically devoid of secreted siderophores. Thus, HPLC-MS analyses fully confirmed the roles of *SID1* and *NPS6* in the siderophore biosynthesis pathway and showed that targeted deletion was successful.

In several fungi, iron sufficiency is indispensable for asexual sporulation, vegetative growth and ROS tolerance (Oide *et al.*, 2006). Although two high-affinity iron uptake systems, i.e. siderophore-mediated iron acquisition and reductive iron assimilation, exist, decreasing iron availability caused by increasing concentrations of BPS in the growth medium led to dramatically decreased conidiation rates of the WT strain (Fig. 3A). Conceivably, Δ*sid1* mutants were unable to produce conidia (Fig. 3B);

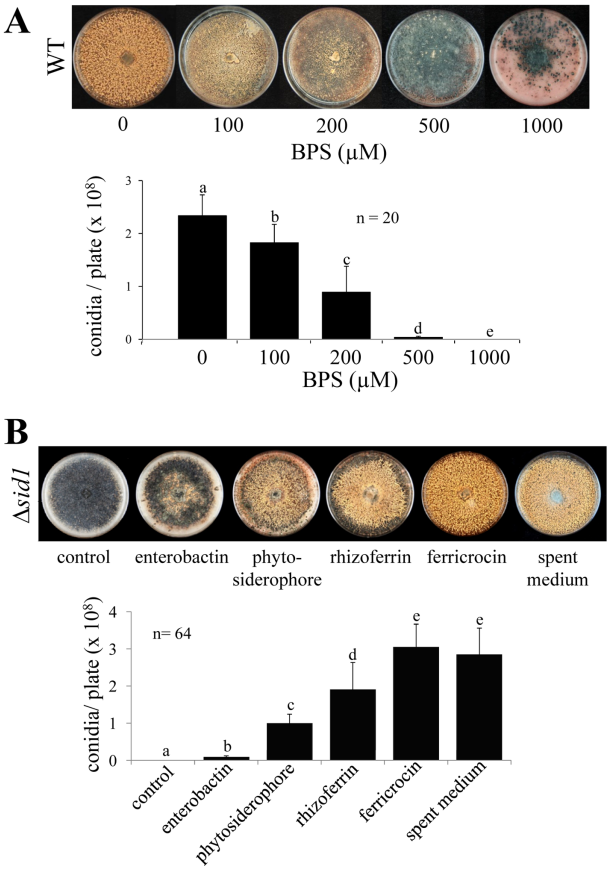

Fig. 3. Effect of iron limitation on conidiation of *C. graminicola*.
A. The WT strain CgM2 showed decreased growth and conidiation rates at increasing BPS concentrations in OMA medium.
B. Supplementing the growth medium with different types of siderophores partially or fully restored conidiation of the Δ*sid1* strain. The hydroxamate type siderophore ferricrocin or the filtrate of CgM2 spent medium fully complemented conidiation rates, whereas the bacterial siderophore enterobactin and phytosiderophores only partially restored conidiation.
Different letters represent significant difference groups ($P < 0.001$).

strains harbouring an ectopically integrated *SID1* deletion cassette were indistinguishable from the WT strain (Fig. S6). Addition of enterobactin, an archetype bacterial siderophore (Raymond and Carrano, 1979) did not restore conidiation, and supplementing oat meal agar (OMA) with a mix of mugineic acid-type phytosiderophores (Meda *et al.*, 2007) or with rhizoferrin, the siderophore originally identified in *Rhizopus microsporus* (Drechsel *et al.*, 1991), only partially restored conidiation. However, the intracellular siderophore ferricrocin as well as spent medium of *C. graminicola*, containing coprogen, coprogen B, and methyl-coprogen B, fully restored conidiation (Fig. 3B).

BPS-induced iron deficiency strongly reduced growth rates of both siderophore mutants generated in this study, Δ*sid1* and Δ*nps6*, as compared to the WT strain and strains ectopically harbouring the cassettes designed to delete the *SID1* or *NPS6* gene respectively (Fig. 4). Likewise, sensitivity to ROS, either H_2O_2 or superoxide, generated by addition of rose bengal to the growth medium and incubation of plates under light, was severely increased in both mutants (Fig. 4). As the strains with the ectopically integrated *SID1* or *NPS6* deletion cassettes did not differ from the WT with respect to growth rate under iron-deficient or -sufficient conditions as well as sensitivity to ROS, only the ectopic strain harbouring the *SID1* deletion cassette was used side by side with the WT strain as a control in further experiments.

Interestingly, Δ*nps6* strains showed no conidiation after 2 and sparse conidiation after 3 weeks of incubation. Supplementing the growth medium with the siderophore coprogen restored conidiation of Δ*nps6* strains (Fig. 5A). Increased magnification revealed that salmon-coloured

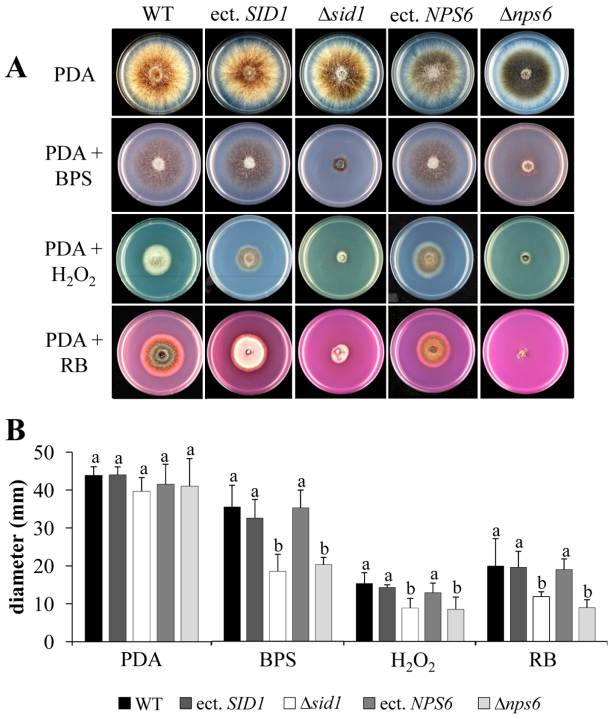

Fig. 4. Effect of iron limitation and reactive oxygen species (ROS) on growth rates of the WT, Δ*sid1* and Δ*nps6* strains of *C. graminicola*.
A. Growth and colony phenotype of the WT strain and the Δ*sid1* mutant and its corresponding ectopic strain (ect. *SID1*), as well as of the Δ*nps6* mutant and its corresponding ectopic strain (ect. *NPS6*) on potato dextrose agar (PDA), PDA containing 100 µM BPS (BPS), 0.01% H_2O_2 (H_2O_2) or 100 µg ml^{-1} of the singlet oxygen-generating agent rose bengal (RB). No differences between WT and the ectopic strains were observed, but Δ*sid1* and Δ*nps6* showed reduced growth under iron-limited condition and were hypersensitive to ROS.
B. Quantitative growth assays show that both BPS and ROS significantly affect growth of Δ*sid1* and Δ*nps6* mutants. Different letters represent significance groups at $P = 0.001$. Bar = + SD, $n = 4$.
The growth rates were measured and photos were taken 4 DPI (PDA, BPS and H_2O_2) and 13 DPI (RB).

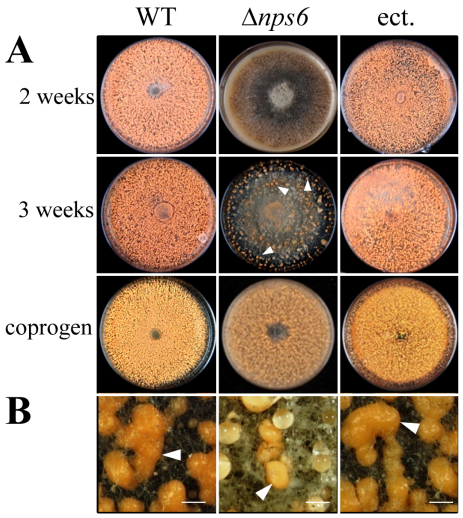

Fig. 5. Phenotype of Δ*nps6* strains of *C. graminicola*.
A. The *C. graminicola* Δ*nps6* strain showed delayed growth rates and reduced rates of formation of acervuli (compare Δ*nps6* frown for 2 and 3 weeks; white arrowheads indicate acervuli) and conidiation in comparison to the WT and ectopic strains (ect.). The addition of coprogen complemented formation of acervuli and conidiation in Δ*nps6* strains.
B. In comparison to WT and ectopic strains, Δ*nps6* strains formed small acervuli (arrowhead).
Bars are 200 μm.

asexual fruiting bodies called acervuli were formed by the WT, by Δ*nps6* strains, and by ectopic transformants (Fig. 5B, arrowheads).

In liquid media spores formed by Δ*sid1* and Δ*nps6* strains exhibited defective shapes (Fig. S7A). Conidia of Δ*sid1* and Δ*nps6* strains grown in liquid complete medium (CM) were significantly smaller than those produced by the WT strain and strains harbouring an ectopically integrated deletion cassette (Fig. S7B).

These data demonstrate that siderophore-mediated iron uptake is required for conidiation.

Siderophore biosynthesis genes are required for cell wall integrity, appressorial penetration and full virulence

Efficient competitive iron uptake by fungal hyphae invading a host plant is required for virulence (Haas *et al*., 2008; Albarouki and Deising, 2013). To test whether siderophore-mediated iron uptake is also required for virulence of *C. graminicola*, we inoculated non-wounded and wounded maize leaf segments as well as intact plants with falcate or oval conidia of the WT strain and of Δ*sid1* and Δ*nps6* deletion strains. Both falcate and oval conidia are able to differentiate melanized appressoria and to infect plants through intact surfaces. All strains formed oval conidia in liquid media without additional supply of iron. On OMA plates, the mutants required the addition of 100 μM $Fe^{(III)}$-EDTA to form falcate conidia (Fig. S6). On non-wounded leaves, Δ*sid1* and Δ*nps6* strains were unable to cause major disease symptoms and were dramatically reduced in virulence (Fig. 6A). The WT strain and strains harbouring an ectopic copy of the *SID1* deletion cassette caused strong symptoms. On wounded leaves, where the fungus omits formation of biotrophic infection structures and directly differentiates necrotrophic hyphae, the WT and the strain harbouring an ectopically integrated deletion cassette showed severe disease symptoms. In comparison with these strains, disease symptoms caused by Δ*sid1* and the Δ*nps6* strains were weaker. Mock-inoculated leaves did not show any symptoms (Fig. 6A). On leaves of intact plants, the WT strain and the strain harbouring an ectopically integrated deletion cassette, but not the Δ*sid1* and Δ*nps6* mutants, caused disease symptoms (Fig. 6A). These data were fully confirmed by qPCR analyses (Fig. 6B). Studying rates of formation of pre-penetration infection structures revealed that germination and appressorium differentiation rates, including melanization, were reduced in both Δ*sid1* and Δ*nps6* deletion strains. Strains carrying an ectopically integrated deletion cassette exhibited appressorium differentiation rates comparable to that of the WT strain (Fig. 6C). However, appressoria that were able to invade the plant differentiated secondary hyphae *in planta* (Fig. 6D). Although the secondary hyphae formed by Δ*sid1* and Δ*nps6* deletion strains were morphologically comparable to those formed by the WT and ectopic strains (Fig. 6D), they showed growth retardation (Fig. 6B). Therefore, reduced virulence of Δ*sid1* and Δ*nps6* strains is due to both, a penetration defect and reduced growth rates of spreading of necrotrophic secondary hyphae, strongly suggesting that siderophores are required for necrotrophic development.

While the WT strains and the strain harbouring an ectopically integrated deletion construct formed massively sporulating acervuli, the Δ*sid1* and Δ*nps6* strains only differentiated initials of acervuli and dramatically reduced spore numbers on both non-wounded and wounded leaves (Fig. S8).

Iron deficiency activates the cell wall integrity pathway in the mammalian pathogen *A. fumigatus* (Jain *et al*., 2011), and mutants of *C. graminicola* deficient in the ferroxidase *FET3-1* and reductive iron assimilation exhibit dramatically reduced class V chitin synthase transcript abundance, severe appressorial cell wall defects and reduced penetration rates (Albarouki and Deising, 2013). In order to address the question as to whether siderophore mutants exhibit infection structure abnormalities, we investigated *on planta* differentiation of infection structures microscopically. Amazingly, while conidia (Fig. 7A, WT, white arrowhead) of the WT strain germinated and differentiated intact melanized appressoria (Fig. 7A, WT, black arrowheads), approximately 50% of the conidia (Fig. 7A, Δ*sid1*, white arrows) and appressoria (Fig. 7A,

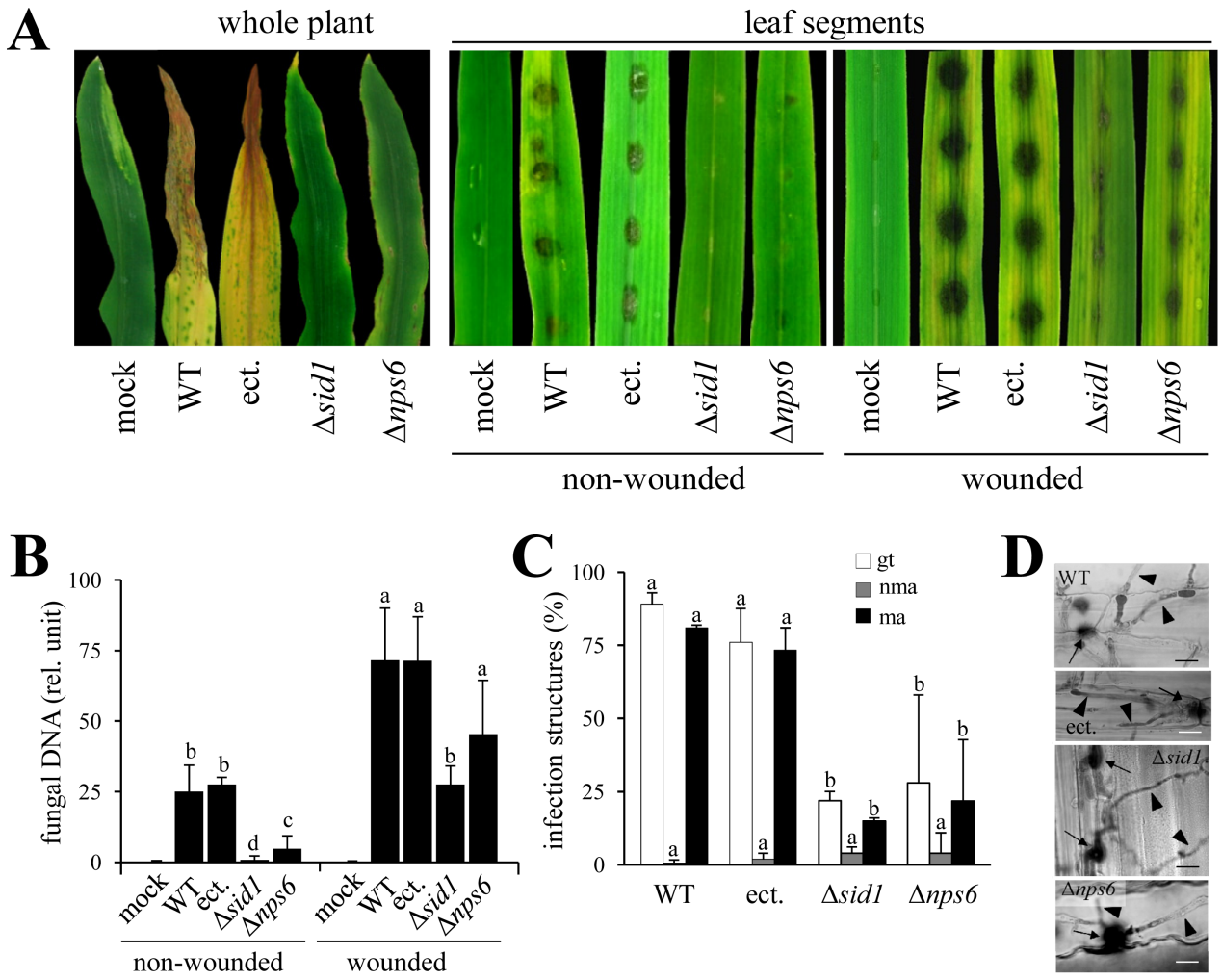

Fig. 6. Virulence of the WT, ectopic, Δ*sid1* and Δ*nps6* strains.
A. Virulence assay on non-wounded detached leaves (4 DPI) showed that WT and ectopic (ect.) strains, but not the representative Δ*sid1* and Δ*nps6* strains, caused the anthracnose symptoms. On wounded leaf segments, Δ*nps6* and Δ*sid1* were able to colonize the leaf tissue, but symptom severity was reduced, as compared with symptoms caused by WT and ectopic strains. On intact whole plants, Δ*sid1* and Δ*nps6* strains were unable to cause disease symptoms.
B. Quantification of fungal mass in infected leaves by qPCR at 4 DPI. Error bars are standard deviations. Different letters represent different significance groups ($P \leq 0.001$, $n = 3$).
C. Differentiation of infection structures on the plant surface by the WT strain, an ectopic strain (ect.), and Δ*sid1* and Δ*nps6* strains at 24 HPI. White bars, germinated conidia; grey bars, non-melanized appressoria; black bars, melanized appressoria. Error bars are standard deviations. Different letters represent different significance groups ($P \leq 0.001$, $n = 1200$).
D. Microscopical analyses of the WT strain, an ectopic strain (ect.), and Δ*sid1* and Δ*nps6* strains were done at 48 HPI; arrows, appressoria; arrowheads, necrotrophic secondary hyphae. Bar = 10 μm.

Δ*nps6*, black arrows) of the mutants lysed and released their cytoplasm onto the plant surface (Fig. 7A, Δ*sid1* and Δ*nps6*, white arrows). Transformants with an ectopically integrated deletion cassette differentiated intact infection cells (data not shown).

In order to confirm cell wall defects in both Δ*sid1* and Δ*nps6* mutants, we performed protoplasting experiments with oval conidia collected from liquid growth medium (Fig. 7B). In both mutants, approximately 40% of the conidia had protoplasted one h after incubation in osmotically stabilized solution containing lysing enzymes. After three h, more than 80% of the conidia of the mutants, but only ~ 8% of the WT conidia and ~ 13% of the conidia of the ectopic strain had protoplasted (Fig. 7B), clearly indicating cell wall defects of the Δ*sid1* and Δ*nps6* mutants.

In Δ*sid1* mutants, which do not synthesize any siderophores, transcript abundances of genes encoding enzymes forming structural cell wall polymers, i.e. the three chitin synthase genes *CHS1*, *CHSIII* and *CHSV*, as well as the β-1,3-glucan synthase gene *GLS1*, were quan-

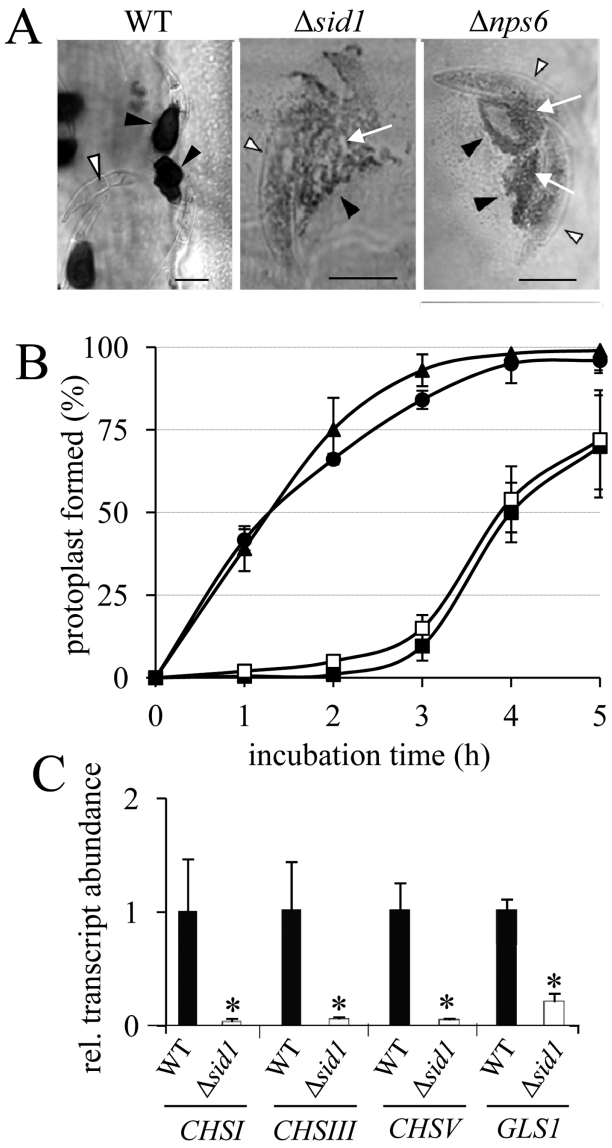

Fig. 7. Δ*sid1* and Δ*nps6* mutants exhibit severe cell wall defects, hypersensitivity to cell wall-degrading enzymes and altered transcript abundances of genes involved in cell wall biogenesis.
A. Conidia (white arrowheads) and appressoria (black arrowheads) of Δ*sid1* and Δ*nps6* mutants lysed and released cytoplasm (black arrowhead) onto maize surface 24 h after inoculation, whereas the WT strain formed melanized dome-shaped appressoria (ap). Bars = 10 μm.
B. Protoplasting efficiency assay show that oval conidia of Δ*sid1* (black triangles), Δ*nps6* (black circles), strains released protoplasts much faster than those of the WT (black squares) and the ectopic strain (white squares). Three individual replicates were counted of each strain, with 100 conidia each at each time point. Bars represent ± SD.
C. Transcript abundance of the chitin synthase genes *CHSI*, *CHSIII* and *CHSV* and the β-1,3-glucan synthase gene *GLS1* in appressoria of WT and Δ*sid1* strains differentiated on polypropylene sheets. Asterisks indicate significant difference between WT and Δ*sid1* ($P \leq 0.001$). Bars represent + SD, $n = 3$.

tified. Transcript concentrations of all of these genes were severely reduced in Δ*sid1* mutants, as compared to the WT strain (Fig. 7C).

Collectively, these data show that siderophore-mediated iron uptake is required for cell wall integrity of pre-penetration differentiated infection structures and for full virulence.

Biotrophy-specific downregulation of biosynthesis and uptake of siderophores is required for modulation of plant defence responses

Comparison of high-affinity iron acquisition pathways in pathogenic fungi differing in lifestyle suggested that biotrophs utilize reductive iron assimilation, whereas necrotrophs employ siderophore mediated iron uptake (Haas *et al.*, 2008). We performed infection cell-specific gene expression studies, taking advantage of transformants harbouring the *eGFP* fusions with the *SID1* (*SID1*:*eGFP*) as well as with the *SIT1* gene (*SIT1*:*eGFP*). Out of four predicted siderophore uptake transporters present in the genome of *C. graminicola*, *SIT1* is the most strongly transcribed (O'Connell *et al.*, 2012). eGFP tagging is required to investigate infection cell-specific regulation of expression of individual genes, as differentiation of infection structures of this fungus does not occur in a sufficiently synchronized manner to employ qRT-PCR. Appressoria of *SID1*:*eGFP* strains fluoresced strongly on the maize cuticle [Fig. 8A, 24 hours post inoculation (HPI), ap]. Surprisingly, immediately at penetration of the plant cell wall eGFP fluorescence disappeared completely in biotrophic primary hyphae (Fig. 8A, 36 HPI, ph). At later stages of pathogenesis, i.e. when the fungus had switched to destructive necrotrophic development, intensive eGFP fluorescence re-appeared in secondary hyphae (Fig. 8A, 72 HPI, sh). Strong eGFP fluorescence was also observed in secondary hyphae at 96 HPI and in acervuli initials (Fig. 8A, 96 HPI, sh and ai), as well as in conidia newly formed in the acervulus (Fig. 8A, 120 HPI, co and av).

In *SIT1*:*eGFP* strains, conidia and germ tubes fluoresced, but no fluorescence was observed in appressoria (Fig. 8B, 24 HPI; co, gt, ap). As in the *SID1*:*eGFP* strain, no fluorescence was seen in biotrophic infection vesicles and in primary hyphae (Fig. 8B, 36 HPI, iv, ph), but fluorescence re-occurred in secondary hyphae (Fig. 8B, 72–120 HPI, sh). Sterigmata did neither fluoresce in *SID1*:*eGFP* nor in *SIT1*:*eGFP* strains (Fig. 8A and B, 120 HPI, st). In contrast, *FET3-1*:*eGFP* strains showed strong fluorescence of biotrophic infection structures (Fig. 8C, 36 HPI, ph), and fluorescence rapidly disappeared when necrotrophic secondary hyphae formed (Fig. 8C, 72 HPI, sh). Importantly, virulence of all eGFP strains used did not differ from that of the WT strain (Fig. S3H, and Albarouki and Deising, 2013).

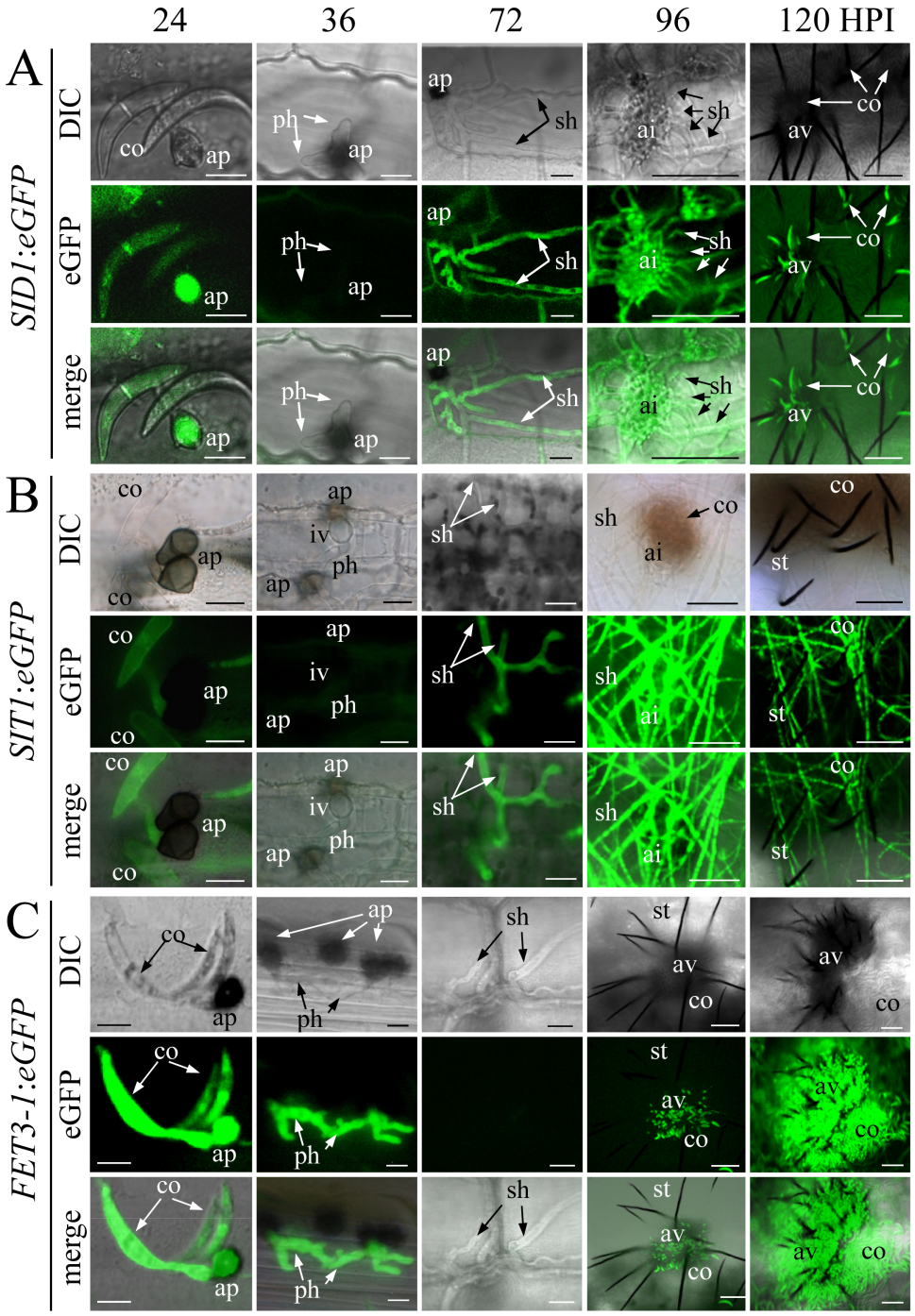

Fig. 8. Infection structure-specific expression of the siderophore synthesis gene *SID1* and the siderophore transporter gene *SIT1*
A. Expression of *SID1* was assessed in a *C. graminicola* replacement strain harbouring a *SID1:eGFP* fusion construct. The *SID1* expression is downregulated during the biotrophic phase (36 HPI) and occurred again during the following necrotrophic phase.
B. Expression of *SIT1* as assessed in a *SIT1:eGFP* strain. The expression of the *SIT1* gene perfectly matches the expression of *SID1* in A.
C. Expression of *FET3-1* was assessed in a *C. graminicola* replacement strain harbouring a *FET3-1:eGFP* fusion construct. *FET3-1* is expressed in infection structures formed on the plant surface and during biotrophy.
ap, appressorium; co, conidium; ph, primary hypha; sh, secondary hypha; ai, acervulus initial; av, acervulus. iv, infection vesicle; st, sterigma. Bars, 24–72 HPI = 10 μm, 96–120 HPI = 50 μm.

Cell type-specific expression of *SID1*, *SIT1* and *FET3-1* clearly visualized complementary employment and lifestyle specificity of the two high-affinity iron uptake strategies. Based on these data we hypothesized that siderophore secretion during biotrophic development may impose a significant disadvantage to the pathogen. Bacterial siderophores have been shown to activate transcription of ferritin genes, and as sequestration of iron by these proteins led to reduced pathogen growth, activation of ferritin genes has been regarded as a plant defence response (Expert, 1999; Dellagi *et al*., 2009; Kieu *et al*., 2012). Greenshields *et al*. (2007) hypothesized that defence responses in plants may also be modulated by fungal siderophores. As simultaneous overexpression of all genes involved in the siderophore biosynthetic and secretory pathway in *C. graminicola* is difficult to accomplish, we decided to infiltrate coprogen, one of the siderophores secreted by this fungus, into maize leaves, and to subsequently inoculate the infiltrated leaves with fungal conidia.

Generation of H_2O_2 is among the fastest defence responses initiated after perception of pathogen ingress. To investigate whether an H_2O_2 response was induced upon infiltration of maize leaves with coprogen, we visualized H_2O_2 by 3,3′diaminobenzidine (DAB) staining (De Neergaard, 1997). In order to discriminate between defence responses induced by coprogen and iron scavenging, leaves were infiltrated with both desferri-coprogen and iron-loaded coprogen (Fe-coprogen) as well as with EDTA as a further control. To test for responses induced by the infiltration process, infiltration was also performed with sterile distilled water. In non-inoculated leaves, no H_2O_2 formation was detected, irrespective of whether leaves were non-infiltrated, water-, EDTA- or siderophore-infiltrated (Fig. 9A). However, at 48 HPI with *C. graminicola*, i.e. when the fungus had established biotrophic hyphae, a dramatic H_2O_2 response was specifically observed in coprogen-pretreated leaves, independent of whether desferri- or Fe-coprogen had been used to infiltrate leaves (Fig. 9A). Importantly, only the coprogen-infiltrated leaf area attacked by melanized appressoria (Fig. 9A, middle panel) showed a DAB-positive response, whereas DAB staining at the margins of the inoculation site was negligible. Under supply of desferri- and Fe-coprogen, most host cells decorated with a fungal appressorium (Fig. 9A, white asterisk) showed strong DAB staining (Fig. 9A, black asterisk) as well as intensive cell wall staining (Fig. 9A, arrowheads). None of the other treatments tested elicited a H_2O_2 response (Fig. 9A). These observations suggest that coprogen, but not iron scavenging or mechanical stress exerted by the infiltration process, pre-conditioned the leaf to respond to subsequent infection by *C. graminicola*.

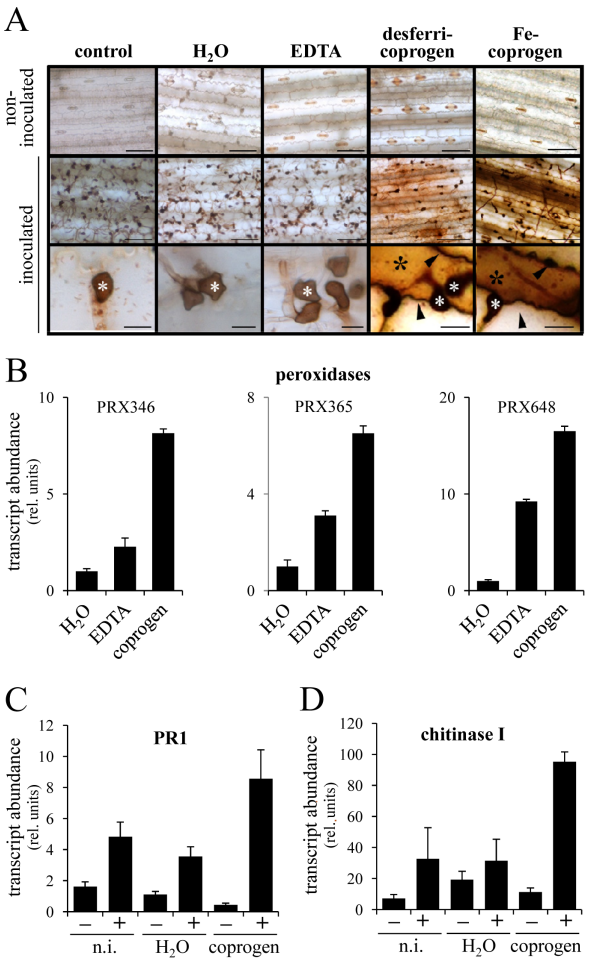

Fig. 9. Coprogen modulates plant defence responses.
A. DAB staining of non-inoculated and inoculated leaves infiltrated with H_2O, EDTA, desferri-coprogen or iron-loaded coprogen (Fe-coprogen). Untreated leaves served as controls. Bars = 100 μm (upper and middle panel) and 10 μm (lower panel).
B. Transcript abundance of genes encoding the maize peroxidases PRX346 (GRMZM2G093346); PRX365 (GRMZM2G117365); and PRX648 (GRMZM2G144648) of water-, EDTA- and coprogen-infiltrated leaves at 48 HPI with the WT strain. Error bars are + standard deviations; $n = 3$.
C and D. Transcript abundance of maize defence marker genes encoding pathogenesis-related protein 1 (PR1) and chitinase I after 48 HPI; n.i., non-infiltrated; H_2O, water-infiltrated; coprogen, coprogen-infiltrated; –, non-inoculated; +, inoculated with the *C. graminicola* WT strain. Error bars are + standard deviations; $n = 3$.

Furthermore, also on the transcript level a strong modulation of defence responses by coprogen was identified. Infiltration of leaves with desferri-coprogen, followed by *C. graminicola* infection, did not only considerably upregulate the transcript abundance of three genes encoding cell wall-localized peroxidase, which use H_2O_2 as a co-substrate, e.g. for lignification of cell walls (Fig. 9B), but also of genes encoding classical PR proteins such as PR1 and a secreted type-I chitinase

(Figs. 9C and D). Peroxidase genes were also activated to some extent in EDTA-infiltrated leaves (Fig. 9B).

Taken together, these data suggest that the siderophore coprogen acts as an immunomodulating compound, and that the hemibiotroph *C. graminicola* downregulates biosynthesis and secretion of siderophores during biotrophic development in order to evade plant immune responses such as H_2O_2 formation, cell wall reinforcement and activation of PR gene expression.

Discussion

Synthesis of immunomodulating siderophores is downregulated in biotrophic fungal infection structures to avoid initiation of defence responses in maize

Biotrophy-specific expression of genes of *C. graminicola* involved in reductive iron assimilation (Albarouki and Deising, 2013) raised the question whether either one of the two iron acquisition strategies bears advantages or disadvantages at certain stages of pathogenesis. In this article we show that the expression of the key gene of siderophore biosynthesis, *SID1*, as well as of the siderophore transporter *SIT1* is rigorously downregulated during biotrophic development of the maize anthracnose fungus *C. graminicola*, but strongly expressed during necrotrophy (Fig. 8). Restriction of siderophore-mediated iron uptake to necrotrophic infection structures brought up the hypothesis that secretion of siderophores into the narrow interfacial matrix surrounding biotrophic infection structures may impose a significant disadvantage to this pathogen during biotrophic development.

An adverse role of siderophores in plant infection was suggested by studies involving bacterial plant pathogens, which showed that siderophores may indirectly immunomodulate plants. In *Arabidopsis thaliana*, the gene *FER1* encoding the iron-binding protein ferritin, is massively activated after infection with the WT strain of the enterobacterium *Erwinia chrysanthemi*. This bacterium secretes the monocatecholate-type siderophore chrysobactin as well as the citrate-derived siderophore achromobactin (Expert, 2005; Boughammoura *et al.*, 2007). In contrast, chrysobactin- and achromobactin-deficient mutants of *E. chrysanthemi* did not transcriptionally activate *FER1*. Furthermore, significant activation of *FER1* occurred in *Arabidopsis* leaves infiltrated with 100 μM chrysobactin, but not in leaves infiltrated with the iron-loaded form of this siderophore, and similar responses to the siderophore desferrioxamine and to its ferric complex have been observed (Dellagi *et al.*, 2005). Since in these experiments alternative iron-complexing agents such as EDTA were not tested, it remained unclear to what extent siderophor-mediated ferritin regulation reflects a consequence of altered cytosolic iron availabilities in the host cell or whether siderophores may directly induce defence responses.

Our present study suggests that a fungal siderophore acts as an immunomodulating agent. Infiltration of maize leaves with coprogen, one of the secreted siderophores of *C. graminicola*, without subsequent inoculation, did neither induce formation of H_2O_2, nor induce transcription of genes encoding pathogenesis-related proteins such as PR1 and chitinases I, which are involved in broad spectrum disease resistance. However, when coprogen-infiltrated leaves were inoculated with *C. graminicola*, massive DAB staining was observed at 48 HPI, i.e. when the fungus had established biotrophic hyphae, and the H_2O_2 response was spatially associated with those cells attacked by the pathogen. This H_2O_2 response did not only occur in leaves infiltrated with desferri-coprogen, but also in leaves infiltrated with the iron-loaded siderophore (Fig. 9A). Neither non-infiltrated control leaves, nor leaves infiltrated with H_2O or leaves infiltrated with the iron-complexing agent EDTA showed an H_2O_2 response, irrespective of whether or not leaves had been inoculated. As H_2O_2 is a co-substrate for peroxidase-mediated cell wall re-enforcement, we analysed the transcript abundance of three cell wall-localized peroxidase genes of maize. Transcript abundance was clearly increased in coprogen pre-infiltrated infected leaves, as compared with infected leaves that had previously been infiltrated with H_2O (Fig. 9B). Moreover, inoculation with *C. graminicola* significantly increased PR1 and class I chitinase transcript levels in coprogen-infiltrated, but not in H_2O infiltrated or non-infiltrated control leaves (Fig. 9C and D). Collectively, these data strongly suggest that the siderophore coprogen modulates broad spectrum defence responses of maize and can therefore be regarded as a priming agent (Conrath, 2011). Interestingly, in various plants, including barley (*Hordeum vulgare*), bean (*Phaseolus vulgaris*) and potato (*Solanum tuberosum*) priming was accomplished by applying spent culture filtrate of *Bacillus subtilis* (B50) but not by applying culture fluid harvested during the logarithmic growth phase. Components in the spent culture filtrate bound iron, suggesting that bacterial siderophores were the active compounds. Indeed, spent media contain high concentrations of siderophores, as iron is quickly consumed and represents a limiting factor for microbial growth (Letendre and Gibbons, 1985). Interestingly, induced resistance was only active against biotrophs such as the barley powdery mildew and the bean rust fungus, and against *Phytophthora infestans* during biotrophic stages of pathogenesis (von Alten and Schönbeck, 1986; U. Steiner-Stenzel, INRES, University of Bonn, Germany, pers. comm.).

Biotrophy-specific downregulation of siderophore biosynthesis appears to be required for evasion of defence responses. Comparably, in *C. graminicola* biotrophy-

specific downregulation of formation of the structural cell wall component β-1,3-glucan, representing a PAMP, is required for evading defence responses in maize and for establishing a compatible parasitic interaction (Oliveira-Garcia and Deising, 2013). Thus, in this fungus the expression of genes, the products of which may contribute to recognition of the pathogen appear to be restricted to infection structures not developing in intimate contact with the plant plasma membrane.

Siderophore-mediated iron uptake is indispensable for cell wall integrity, asexual sporulation, and hyphal growth

In *C. graminicola*, like in the vast majority of pathogens analysed so far, high-affinity iron uptake systems are indispensable not only for hyphal growth under iron-limited conditions, but also for asexual sporulation (Eichhorn *et al*., 2006; Oide *et al*., 2006; Schrettl *et al*., 2007) (Figs 3 and 5). Indeed, in plant pathogenic fungi sporulation is a key requirement for spreading of diseases caused by air-borne pathogens such as rust fungi and powdery mildews (Limpert *et al*., 1999; Hovmoller *et al*., 2008; Singh *et al*., 2011). Although long-distance dispersal of spores by water is thought to be unlikely (Bärlocher, 2009), spores produced in acervuli, which are embedded into a mucilaginous matrix and normally are dispersed by rain events, can be wind-dispersed over large distances on dried fragments of their host leaves (Nicholson and Moraes, 1980; Bergstrom and Nicholson, 1999).

In order to identify genes required for conidiation, early work in *A. nidulans* employed a subtractive hybridization procedure called cascade hybridization to purify cDNAs complementary to poly(A) + RNA sequences. The results suggested that ~ 1000 mRNAs are present in conidiating cultures, but not in vegetative hyphae (Timberlake, 1980; 1990). More recent work analysed transcriptional changes in the transition from vegetative cells to asexual sporulation, taking advantage of Illumina-based RNA sequencing. Interestingly, ~ 20% of the genes were significantly altered at the transcriptional level, with 2035 genes being downregulated, and only 187 upregulated. Among the top 20 upregulated genes were genes encoding proteins which are involved in cell wall biogenesis, i.e. the putative β-1,3-transglycosidase gelD, a putative endo-mannanase, and two hydrophobins, including rodA (Garzia *et al*., 2013). Notably, although not among the top 20 upregulated genes, the *SID1* orthologue *SidA* was significantly upregulated during asexual sporulation (Garzia *et al*., 2013). In line, in *A. fumigatus* the intracellular siderophore ferricrocin has been shown to be involved in intracellular iron trafficking, which is particularly crucial for conidiation (Wallner *et al*., 2009). Under iron deficiency, genes required for purine biosynthesis are downregulated, and although no known iron-dependent enzymes have been identified in this pathway in *Saccharomyces cerevisiae*, purine biosynthesis is an iron-dependent process in most organisms, including yeast and likely also filamentous fungi (Philpott and Protchenko, 2008). Therefore, iron limitation must have a drastic effect on transcription of genes required at specific stages of morphogenesis, and this likely holds true for genes involved in cell wall biogenesis in conidia and fungal infection structures (Garzia *et al*., 2013; Oliveira-Garcia and Deising, 2013).

Furthermore, in the human pathogen *Candida albicans* 11 genes encoding glycosylphosphatidylinositol (GPI)-anchored proteins, including *RBT5*, as well as several cell wall proteins, including *BGL2*, encoding a β-1,3-glucan transferase and *PIR1*, encoding a structural cell wall protein, are controlled by iron availability (Lan *et al*., 2004). The expression of the *RBT5* gene of *C. albicans*, required for cell wall integrity, is regulated by the iron-responsive GATA-like factor Sfu1p (Mishra *et al*., 2011). Interestingly, also in *C. graminicola* cell wall integrity may be regulated by an iron-responsive GATA-like factor, as GATA binding sites are present at two positions (–163 and –431) of the 5′-noncoding region of the chitin synthase gene *CHSV* and at two positions (–17 and –282) of the 5′-noncoding region of the β-1,3-glucan synthase gene *GLS1*. Thus, control of cell wall biogenesis genes of *C. graminicola* might be administered by homologues of the GATA factor SreA, possibly in tight interplay with repressors such as Hap-like CCAAT binding complexes known from filamentous fungi such as *A. fumigatus* (Brakhage *et al*., 1999; Hortschansky *et al*., 2007). The presence of putative Hap-like binding complexes at position –231, –481 and –490 in the 5′-noncoding regions of *CHSI*, *CHSV* and *GLS1* genes, respectively, supports this assumption. Furthermore, in *A. fumigatus* the MAP kinase MpkA controls cell wall integrity, iron adaptation and oxidative stress response (Valiante *et al*., 2009; Jain *et al*., 2011). Accordingly, dramatic iron limitation in Δ*sid1* or Δ*nps6* mutants on the plant surface may lead to activation of MpkA, which, in turn, might activate a repressor of genes involved in cell wall biogenesis, eventually causing lysis of spores, germ tubes or appressoria differentiated on the plant cuticle (Fig 7A, Δ*sid1* and Δ*nps6*) (Jain *et al*., 2011).

Indeed, in *sid1* mutants of *C. graminicola* the transcript abundance of three different genes encoding chitin synthases, i.e. *CHSI*, *CHSIII* and *CHSV*, as well as of the β-1,3-glucan synthase gene *GLS1* were clearly downregulated (Fig. 7C). As cell wall biogenesis is of particular importance during germination of conidia and rapid differentiation of infection structures *on planta*, transcription of genes and synthesis of enzymes involved in cell wall biogenesis may be particularly affected by limited availability of purine nucleotides. This may also explain why the

addition of 0.5 mM BPS reduced conidiation by 98% (Fig. 3A). In both Δ*sid1* and Δ*nps6* mutants of *C. graminicola* cell wall defects are clearly visible in conidia and appressoria (Fig. 7A). Also in siderophore-defective mutants of *F. graminearum* and *A. fumigatus* conidiation is dramatically reduced (Schrettl *et al*., 2004; Oide *et al*., 2006).

Thus, as iron limitation causes significant reduction in abundance of fungal spores as well as failure in hyphal growth and infection structure differentiation, iron is not only a key factor for pathogenicity, but also for initiation and spreading of disease in the field.

Perspectives for employing siderophore-mediated iron uptake in plant protection

Our work and that of others has shown that genes encoding siderophore-synthesizing enzymes as well as genes encoding siderophore transporters are active under iron-limiting conditions, including development on the plant surface and/or in the host tissue (Fig. 8) (Jain *et al*., 2011). An excellent example of how siderophores can be used to increase the sensitivity of pathogens to chemical control agents is provided by sideromycins, which are natural siderophore drug conjugates produced by bacteria such as *Actinomyces subtropicus*, *Streptomyces griseoflavus* and *Streptomyces violaceus*. Chemical control of pathogenic bacteria is hampered by limited permeability of their outer membrane for antibiotics. An efficient strategy to overcome this membrane-mediated resistance is the misuse of bacterial iron transport systems by sideromycins (Möllmann *et al*., 2009). Already in 1951, the sideromycin albomycin has been discovered in cultures of *A. subtropicus* (Gause, 1955; Benz *et al*., 1982), whereas *S. violaceus* produces the closely related sideromycin salmycin. Salmycin consists of an amino disaccharide linked to the ferrioxamine B-type siderophore danoxamine via a dicarboxylic spacer. Salmycins are thought to be taken up by hydroxamate transporters, and the antibiotic amino glycoside may be released inside the cell upon hydrolysis (Vértesy *et al*., 1995). Alternatively, it is thought that iron reduction may trigger drug release via an intramolecular cyclization process (Roosenberg and Miller, 2000). Adopting the bacterial strategy of employing microbial high-affinity siderophore uptake systems to introduce natural siderophore drug conjugates, known as the Trojan Horse strategy, synthetic siderophore drug conjugates may be used to control pathogenic bacteria (Heinisch *et al*., 2002; Miller *et al*., 2009). To date, conjugates of siderophores with a variety of commercially available antibiotics with different cellular targets have been developed (Wencewicz *et al*., 2009). It is tempting to speculate whether corresponding conjugates of fungal siderophores with different fungicides, e.g. azoles, dicarboximides or strobilurins, could be used in a corresponding Trojan Horse strategy to combat plant pathogenic fungi.

Alternatively, enzymes involved in siderophore biosynthesis may be used as a target of novel antifungal compounds. For example, the bacterial pathogens *Mycobacterium tuberculosis* and *Yersinia pestis*, causing tuberculosis and plague in man, respectively, use the mycobactin and yersiniabactin siderophores, both of which have salicyl-capped non-ribosomal peptide-polyketide hybrid scaffolds. Small non-hydrolysable molecules such as acyl sulphamoyl adenosides mimic the substrate of the salicylate adenylating enzymes MbtA and YbtE and inhibit siderophore biosynthesis in a non-competitive fashion (Ferreras *et al*., 2005). Adopting this strategy, analogues of substrates of enzymes involved in fungal hydroxamate-type siderophore biosynthesis may be synthesized and tested for their antifungal activity and applicability in plant protection. Thus, the detailed understanding of fungal iron uptake strategies may help to develop novel strategies to combat pathogenic fungi and to improve plant protection.

Experimental procedures

Strains, media and culture condition

The wild-type strain CgM2 of *C. graminicola* was provided by R.L. Nicholson, Purdue University, Indiana. The CgM2 strain was grown on oat meal agar (OMA). The Δ*sid1* and Δ*nps6* were grown on OMA medium supplemented with 100 μM $Fe^{(III)}$-EDTA (Duchefa, Haarlem, the Netherlands). Alternatively, strains were grown in liquid complete medium (Leach *et al*., 1982) in an incubation shaker (Unitron, Infors AG, Bottmingen, Switzerland) at 23°C and 100 r.p.m.

Sensitivity to reactive oxygen species and iron-limiting conditions were tested as described previously (Albarouki and Deising, 2013).

Infection assays

Fourteen-day-old maize (*Z. mays* cv. Nathan; KWS SAAT AG, Einbeck, Germany) plants were used in the infection assays. Quantitative PCR (qPCR) was employed for quantifying fungal mass of the infection sites as described previously (Albarouki and Deising, 2013).

Formation of conidia

The *C. graminicola* wild-type strain produces conidia when grown on OMA plates at 23°C and constant UV-light (TLD36W/08; Philips, Hamburg, Germany). The ability of the WT strain and the corresponding mutants to form conidia was assayed on OMA plates supplemented with different concentration of $FeSO_4$, $FeCl_3$, $Fe^{(III)}$-EDTA, siderophores (i.e. ferricrocin, coprogen, ferrichrome, rhizoferrin, phytosiderophores or enterobactin) or the iron scavenger BPS. Fifty-millimetre plates were filled with 10 ml OMA and inoculated with a

0.4-cm-diameter mycelial block using a cork borer from the front edge of the growing *C. graminicola* strains.

The phytosiderophores used in this study were collected from barley root exudates and purified according to Meda *et al*. (2007). Briefly, barley plants were first grown in iron-sufficient hydroponic solution for 2 weeks. After 1-week pre-culture under iron-deficiency, root exudates were collected daily and pooled. The root exudates were concentrated and prepurified by cation exchange chromatography (Dowex 50 WX column, Serva) and quantified by HPLC.

The plates were incubated at 23°C and constant UV light for 2 weeks. Thereafter, the conidia formed were washed from the plate with 2 ml distilled water, the washing process was repeated three times until the conidia were completely removed from the plate. The washed conidia were collected in 15 ml Falcon tube (Greiner bio-one, Frickenhausen, Germany), and counted in a haemocytometer (Thoma, LO-Laboroptik, Friedrichsdorf, Germany). Four plates were used per strain and growth assays were repeated four times.

Transcript abundance of genes involved in siderophore-mediated iron uptake

Mycelium of *C. graminicola* was grown in CM medium for 4 days. The grown mycelia were filtered through Miracloth (EMD Chemical, Darmstadt, Germany) and washed three times with sterile deionized water (Milli-Q, TKA, Thermo Electron LED GmbH, Niederelbert, Germany) under sterile conditions. Thereafter, 100 mg of the mycelium was transferred into iron free CM medium containing 50 μM of BPS for 2 days. Subsequently, the mycelium was transferred to fresh CM medium containing 0.01 mM or 1 mM ferric ($FeCl_3$), or ferrous ($FeSO_4$) iron, or 50 or 200 μM BPS for additional 2 days.

RNA isolation from *C. graminicola* was done according to Chirgwin *et al*. (1979). Genomic DNA was removed using Turbo DNA free ™ Kit (Life Technology, Darmstadt, Germany). Quantitative RT-PCR (qRT-PCR) was performed as described previously (Albarouki and Deising, 2013). All primers used for quantitative PCR are listed in Supplemental Table S1.

Targeted deletion of SID1 and NPS6 genes of C. graminicola

Deletion cassettes for the *SID1* gene was generated by double-joint PCR (Yu *et al*., 2004). The 5′- and 3′-flanking regions of the *SID1* gene were amplified with the primer combinations SID1-KO-5′-Fw and SID1-KO-5′-Rv, and SID1-KO-3′-Fw and SID1-KO-3′-Rv, and 100 ng of genomic DNA as template. The hygromycin phosphotransferase (*hph*) cassette was amplified from plasmid pAN7-1 (Punt *et al*., 1987), using primers Hyg-Fw and Hyg-Rv. In a second PCR, the 5′- and 3′-flanks were fused with the *hph* cassette, and the complete product was amplified using nested primers SID1-KO-nest-Fw.1 and SID1-KO-nest-Rv.1. The 4519 bp product was cloned into pJET1.2/blunt, yielding pSID1KO. This vector was used as a template to amplify the KO construct using primers SID1-KO-nest-Fw.2 and SID1-KO-nest-Rv.2 primers and transformed into conidial protoplasts as described (Werner *et al*., 2007).

The inactivation of the *NPS6* gene was achieved by a partial deletion of the ORF and substitution by hygromycin resistance cassette. First, a 5912 bp fragment of the *NPS6* was amplified by PCR using primer pairs NPS6-Fw and NPS6-Rv, and cloned into pJET1.2/blunt. The resulting plasmid pNPS6 was digested with the AgeI endonuclease, resulting in the removal of 3229 bp of the ORF. The linearized plasmid was then dephosphorylated. The 2692 bp hygromycin resistance cassette was cut from pAN7-1 using (AgeI/NgoMIV) double digestion and subcloned into the AgeI-digested pNPS6, resulting pNPS6KO. The entire 5.6 Kb KO cassette was amplified from pNPS6KO by PCR using primer pairs NPS6-KO-nest-Fw and NPS6-KO-nest-Rv, and used to transform conidial protoplast.

All PCRs were performed using Phusion High-Fidelity DNA Polymerases (New England Biolabs, County Road, Ipswich, England).

Generation of P_{SID1}:eGFP, SID1:eGFP and SIT1:eGFP fusion constructs, and transformation into C. graminicola

The *eGFP* fragment was amplified by primer pairs EGFP-Fw and EGFP-Rv.1 from the plasmid pFET3-2-eGPF-G418 (Albarouki and Deising, 2013), resulting in a 1300 bp fragment. The SID1 promoter (P_{SID1}) was amplified by primer pairs SID1-Kpn2I-SfiIA-Fw and SID1-DraIII-SfiIB-Rv resulting in a 904 bp fragment. Both PCR fragments were purified and digested using DraIII. The two pieces were then ligated and amplified by PCR using primer pairs SID1-Kpn2I-SfiIA-Fw and EGFP-Rv.1. The resulting P_{SID1}:eGFP construct was then ligated into OliI-digested pNR1 plasmid (Malonek *et al*., 2004) resulting in the plasmid pEB14-eGFP.

The construction of the *SID1*:*eGFP* fusion cassette was mediated by the cloning of *SID1* gene into plasmid pEB14-eGFP. The *SID1* gene was amplified with primer pairs SID1-Kpn2I-SfiIA-Fw and SID1-SfiIB-Rv, and 100 ng of gDNA. The PCR fragment was digested with SfiI and cloned into plasmid pEB14-eGFP. The 5′-SfiI A and 3′-SfiI B overhangs allowed the oriented ligation of the SID1 gene in the frame of *eGFP*. The resulting plasmid pEB14-SID1-eGFP was sequenced and the ORF of the *SID1*:*eGFP* fused gene was confirmed.

To construct the *SIT1*:*eGFP* cassette, the *SIT1* gene was amplified with SIT1-SfiIA-Fw and SIT1-SfiIB-Rv primers. The PCR product was digested with SfiI and cloned into the pEB14-eGFP plasmid in the frame with the *eGFP* gene. The resulting plasmid pEB14-SIT1-eGFP was confirmed by sequencing.

The P_{SID1}:*eGFP*, *SID1*:*eGFP* and *SIT1*:*eGFP* constructs were amplified by PCR, using primers pEB-uni-Fw and pEB-uni-Rv and transformed into conidial protoplasts as described (Werner *et al*., 2007).

All PCRs were performed using Phusion High-Fidelity DNA Polymerases (New England Biolabs, County Road, Ipswich, England).

Construction of the *FET3-1*:*eGFP* strain has been described previously (Albarouki and Deising, 2013).

DNA extraction and genomic Southern blot analyses

Extraction of genomic DNA from vegetative mycelium of *C. graminicola* was done as described (Döbbeling *et al*.,

1997). Five micrograms of genomic DNA was used for Southern blot analyses and digested with either MunI (*SID1*) or EcoRV (NPS6) and separated on a 0.7% (w/v) agarose gel as described before (Albarouki and Deising, 2013).

DIG-dUTP-labelled probes were generated by PCR, using primers Hyg-prob-Fw and SID1-KO-nest.Rv.2 and plasmid pSID1KO as template (*SID1*), or primers Hyg-prob-Fw and NPS6-KO-nest-Rv and plasmid pNPS6KO (*NPS6*). *Taq* polymerase was used for amplifying probes. Hybridization and probe detection was carried out as described (Roche Diagnostics, Mannheim, Germany), and membranes were exposed to Hyperfilm ECL X-ray film (Amersham Pharmacia Biotech Europe, Freiburg, Germany).

Siderophore analysis

Colletotrichum graminicola strains were grown in CM medium in an incubation shaker (Unitron, Infors AG, Bottmingen, Switzerland) at 25°C and 100 r.p.m. for 7–10 days. Then the fungal mycelia were filtrated under sterile conditions through Miracloth filter (EMD Chemical, Darmstadt, Germany) and washed three times with H_2O_{bidest}. The fungal mycelia were then dried gently with sterile filter paper (601A Carl Roth, Karlsruhe, Germany) and weighted. One gram fresh weight of fungal mycelium was used to inoculate 150 ml of Sundström minimal medium (Sundström, 1964) in 500 ml Erlenmeyer flasks. The inocula were grown at 25°C for an additional 10 days. The mycelia and the growth broth were separated by filtration (601A Carl Roth, Karlsruhe, Germany).

For analysis of intracellular siderophores, the mycelium was freeze dried. One hundred milligrams were homogenized in 1.8 ml of 0.05 M sodium-phosphate buffer, pH 6.5. One ml of the generated cell extract was iron saturated with 100 µl of 100 mM $FeSO_4$ and mixed thoroughly. After centrifugation to remove any precipitated iron, 10 µl were applied to reversed phase HPLC.

Extracellular siderophores were analysed from the supernatant obtained after a cultivation period of 10 days. Ten millilitres of each sample were applied to an Amberlite XAD-16 column (Rohm and Haas, Philadelphia, PA, USA) and equilibrated with water. Iron saturation of matrix-bound siderophores was achieved by addition of 100 µl of 100 mM $FeSO_4$. Siderophore-iron complexes were eluted with 2 ml of methanol and collected. Methanol was discarded by speed vacuum centrifugation overnight. The dried pellet was solubilized in 100 µl of water and 10 µl were applied to reversed phase HPLC.

Compounds displaying absorption at 430 nm, which is typical for iron-saturated siderophores, were subjected to mass spectrometry. Determination of the molecular mass of the samples obtained by RP-HPLC was carried out using a LTQ Velos ion trap mass spectrometer (Thermo Fisher Scientific, Vienna, Austria) equipped with an electrospray source (ESI-MS, electrospray ionization mass spectrometry, Vienna, Austria). Samples were dissolved in 50% aqueous methanol containing 0.1% formic acid, and infused directly into the ion source using the syringe pump. The electrospray voltage was set at 4.0 kV and the heated capillary was held at 270°C.

Protoplasting of oval conidia

Oval conidia formed in 0.5 M sucrose medium containing 0.1% yeast extract (Werner *et al*., 2007) were collected and suspended in a protoplast induction solution containing 20 mg ml^{-1} lysing enzymes from *Trichoderma harzianum* (Sigma, Deisenhofen, Germany); 0.1% (v/v) β-mercaptoethanol in 0.7 M NaCl. The suspension was incubated at 30°C and 80 r.p.m. (Unitron, Infors AG, Bottmingen, Switzerland). Protoplasting efficiency was microscopically assessed every hour until the conidia fully protoplasted.

Microscopy

Bright-field and differential interference contrast microscopy were performed using a Nikon Eclipse 90i microscope (Nikon, Düsseldorf, Germany), equipped with DS-5 M camera. Aniline blue and 3,3′-diaminobenzidine (DAB) stainings were performed as described (De Neergaard, 1997).

Fluorescence microscopy was performed, using a Nikon Eclipse 90i confocal laser scanning microscope (Nikon, Düsseldorf, Germany), equipped with D-Eclipse C1-SHV camera and a pinhole diameter of 30 µm. For detection of eGFP fluorescence, an excitation wavelength of 488 nm and a 535/550 nm detection channel were employed.

Fluorescence intensity was measured using the EZ-C1 software (Nikon, Düsseldorf, Germany) as described before (Albarouki and Deising, 2013).

Image processing was done with Adobe Photoshop CS (Adobe Systems, San Jose, CA, USA).

Bioinformatic and prediction tools

In silico sequence analyses, gene deletion, gene fusion and primer construction were made using Clone Manager 9 professional (Sci-Ed., Cary, NC, USA).

Phylogenetic analyses were performed using MEGA4 software (Tamura *et al*., 2007). The evolutionary relationship was analysed using the Minimum Evolution method (Rzhetsky and Nei, 1992), and bootstrap consensus trees were inferred from 1000 replicates (Felsenstein, 1985).

Calculation and statistical analysis of differences between groups were done using the one-way ANOVA test, followed by the Holm-Sidak test at a freedom degree ($P < 0.001$) (Sigma Plot v.11, Systat Software, Erkrath, Germany).

Accession numbers

Accession numbers of Sid1 proteins. Ajellomyces capsulatus (EEH02759.1), *Arthroderma otae* (XP002850162.1), *Aspergillus clavatus* (XP001267710.1), *Aspergillus fumigatus* (XP755103.1), *Aspergillus nidulans* (XP663427.1), *Aspergillus terreus* (XP001209565.1), *Botryotinia fuckeliana* (CCD45292.1), *Claviceps purpurea* (CCE29720.1), *Coccidioides immitis* (XP001247661.1; XP001247172.1), *Coccidioides posadasii* (EFW15727.1, EFW21588.1), *Colletotrichum graminicola* (EFQ31396.1), *Colletotrichum higginsianum* (CCF41271.1), *Fusarium graminearum* (XP385547.1), *Magnaporthe oryzae* (EHA47238.1), *Metarhizium anisopliae* (EFZ02309.1), *Metarhizium acridum* (EFY85959.1),

Mycosphaerella graminicola (XP003855779.1), *Neurospora crassa* (XP960300.2), *Parastagonospora nodorum* (EAT90349.1), *Penicillium chrysogenum* (XP002558960.1), *Puccinia graminis* f. sp. *tritici* (XP003889143.1), *Pyrenophora tritici-repentis* (XP001938606.1; XP001942089.1; XP001932013.1), *Schizosaccharomyces pombe* (CAB72228.1), *Sclerotinia sclerotiorum* (XP001595607.1), *Sordaria macrospora* (XP003346089.1), *Talaromyces stipitatus* (XP002478751.1), *Verticillium alfalfa* (EEY23902.1), *Verticillium dahliae* (EGY14149.1).

Accession numbers of Nps6 proteins. *Ajellomyces capsulatus* (EEH02753.1), *Ajellomyces dermatitidis* (EGE78437.1), *Alternaria alternata* (AFN69082.1), *Alternaria brassicicola* (ABI51983.1), *Aspergillus clavatus* (XP001273566.1), *Aspergillus fumigatus* (EDP53310.1), *Aspergillus flavus* (XP002385307.1), *Bipolaris carbonum* (AFJ97105.1), *Bipolaris oryzae* (ABI51982.1), *Bipolaris sorokiniana* (AER36015.1), *Coccidioides immitis* (EAS36195.2), *Coccidioides posadasii* (XP003065781.1), *Cochliobolus heterostrophus* (AAX09988.1), *Colletotrichum graminicola* (EFQ32921.1), *Colletotrichum gloeosporioides* (ELA26594.1), *Colletotrichum higginsianum* (AFI23576.1), *Fusarium fujikuroi* (CCE73648), *Fusarium graminearum* (XP_383923.1), *Magnaporthe oryzae* (XP003714007.1), *Nectria haematococca* (XP003048492.1), *Schizosaccharomyces pombe* (CAB72227.1), *Trichoderma reesei* (EGR46022.1), *Uncinocarpus reesii* (XP002541830.1), *Ustilago maydis* (AAB93493.1).

Accession numbers of maize (Z. mays*) defence genes.* Pathogenesis-related protein 1 (PR1) (ACG29538.1), chitinase I (ACJ62153.1), GRMZM2G093346 (AFW78948.1), GRMZM2G117365 (AFW81877.1), GRMZM2G144648 (ACG24777.1) and GRMZM2G323731 (AFW80851.1).

Acknowledgements

This work was funded by the Interdisciplinary Center of Crop Plant Research (Interdisziplinäres Zentrum für Nutzpflanzenforschung, IZN, Grant No. Kap.00602, TG 68, project 10). We are indebted to Bettina Tudzynski, University of Münster, Germany, for providing plasmid pNR1. We thank Andrea Beutel, Doris Jany, and Elke Vollmer (Martin-Luther-University University Halle-Wittenberg, Germany) for skilful technical support. E.A. was supported in part by the German Academic Exchange Service (DAAD, Grant No. A/05/55302). Studies by L.S. and H.H. were supported by the Austrian Science Foundation Grant FWF P21643-B11.

References

Albarouki, E., and Deising, H.B. (2013) Infection structure-specific reductive iron assimilation is required for cell wall integrity and full virulence of the maize pathogen *Colletotrichum graminicola*. *Mol Plant Microbe Interact* **26:** 695–708.

von Alten, H., and Schönbeck, F. (1986) The effect of chelating agents on a rust fungus developing on induced resistant plants. In *Iron, Siderophores, and Plant Diseases*. Swinburne, T.R. (ed.). New York and London: Plenum Press, pp. 243–247.

Arosio, P., and Levi, S. (2002) Ferritin, iron homeostasis, and oxidative damage. *Free Radic Biol Med* **33:** 457–463.

Bärlocher, F. (2009) Reproduction and dispersal in aquatic hyphomycetes. *Mycoscience* **50:** 3–8.

Behr, M., Humbeck, K., Hause, G., Deising, H.B., and Wirsel, S.G.R. (2010) The hemibiotroph *Colletotrichum graminicola* locally induces photosynthetically active green islands but globally accelerates senescence on aging maize leaves. *Mol Plant Microbe Interact* **23:** 879–892.

Benz, G., Schröder, T., Kurz, J., Wünsche, C., Karl, W., Steffen, G.J., *et al.* (1982) Konstitution der Deferriform der Albomycine δ_1, δ_2 und ε. *Angew Chem* **94:** 552–553.

Bergstrom, G.C., and Nicholson, R.L. (1999) The biology of corn anthracnose. Knowledge to exploit for improved management. *Plant Dis* **83:** 596–608.

Birch, L.E., and Ruddat, M. (2005) Siderophore accumulation and phytopathogenicity in *Microbotryum violaceum*. *Fungal Genet Biol* **42:** 579–589.

Boughammoura, A., Franza, T., Dellagi, A., Roux, C., Matzanke-Markstein, B., and Expert, D. (2007) Ferritins, bacterial virulence and plant defence. *Biometals* **20:** 347–353.

Brakhage, A.A., Andrianopoulos, A., Kato, M., Steidl, S., Davis, M.A., Tsukagoshi, N., and Hynes, M.J. (1999) HAP-Like CCAAT-binding complexes in filamentous fungi: implications for biotechnology. *Fungal Genet Biol* **27:** 243–252.

Chirgwin, J.M., Przybyla, A.E., MacDonald, R.J., and Rutter, W.J. (1979) Isolation of biologically active ribonucleic acid from sources enriched in ribonuclease. *Biochemistry* **18:** 5294–5299.

Conrath, U. (2011) Molecular aspects of defence priming. *Trends Plant Sci* **16:** 524–531.

De Neergaard, E. (1997) *Methods in Botanical Histopathology*. Copenhagen, Denmark: Kandrups Bogtrykkeri.

Dellagi, A., Rigault, M., Segond, D., Roux, C., Kraepiel, Y., Cellier, F., *et al.* (2005) Siderophore-mediated upregulation of *Arabidopsis ferritin* expression in response to *Erwinia chrysanthemi* infection. *Plant J* **43:** 262–272.

Dellagi, A., Segond, D., Rigault, M., Fagard, M., Simon, C., Saindrenan, P., and Expert, D. (2009) Microbial siderophores exert a subtle role in *Arabidopsis* during infection by manipulating the immune response and the iron status. *Plant Physiol* **150:** 1687–1696.

Döbbeling, U., Böni, R., Häffner, A., Dummer, R., and Burg, G. (1997) Method for simultaneous RNA and DNA isolation from biopsy material, culture cells, plants and bacteria. *Biotechniques* **22:** 88–90.

Drechsel, H., Metzger, J., Freund, S., Jung, G., Boelaert, J.R., and Winkelmann, G. (1991) Rhizoferrin – a novel siderophore from the fungus *Rhizopus microsporus* var. *rhizopodiformis*. *Biometals* **4:** 238–243.

Eichhorn, H., Lessing, F., Winterberg, B., Schirawski, J., Kämper, J., Müller, P., and Kahmann, R. (2006) A ferroxidation/permeation iron uptake system is required for virulence in *Ustilago maydis*. *Plant Cell* **18:** 3332–3345.

Eisendle, M., Oberegger, H., Zadra, I., and Haas, H. (2003) The siderophore system is essential for viability of *Asper-*

gillus nidulans: functional analysis of two genes encoding L-ornithine N^5 monooxygenase (*sidA*) and a non-ribosomal peptide synthetase (*sidC*). *Mol Microbiol* **49:** 359–375.
Expert, D. (1999) Withholding and exchanging iron: interactions between *Erwinia* spp. and their plant hosts. *Annu Rev Phytopathol* **37:** 307–334.
Expert, D. (2005) Genetic regulation of iron in *Erwinia chrysanthemi* as pertains to bacterial virulence. In *Iron Nutrition in Plants and Rhizospheric Microorganisms*. Barton, L., and Abadia, J. (eds). Berlin: Springer, pp. 215–227.
Felsenstein, J. (1985) Confidence limits on phylogenies: an approach using the bootstrap. *Evolution* **39:** 783–791.
Ferreras, J.A., Ryu, J.-S., Di Lello, F., Tan, D.S., and Quadri, L.E.N. (2005) Small-molecule inhibition of siderophore biosynthesis in *Mycobacterium tuberculosis* and *Yersinia pestis*. *Nat Chem Biol* **1:** 29–32.
Garzia, A., Etxebeste, O., Rodríguez-Romero, J., Reinhard Fischer, R., Espeso, E.A., and Ugaldea, U. (2013) Transcriptional changes in the transition from vegetative cells to asexual development in the model fungus *Aspergillus nidulans*. *Eukaryot Cell* **12:** 311–321.
Gause, G.F. (1955) Recent studies on albomycin, a new antibiotic. *Br Med J* **12:** 1177–1179.
Greenshields, D.L., Liu, G., Feng, J., Selvaraj, G., and Wei, Y. (2007) The siderophore biosynthetic gene *SID1*, but not the ferroxidase gene *FET3*, is required for full *Fusarium graminearum* virulence. *Mol Plant Pathol* **8:** 411–421.
Haas, H., Eisendle, M., and Turgeon, B.G. (2008) Siderophores in fungal physiology and virulence. *Annu Rev Phytopathol* **46:** 149–187.
Heinisch, L., Wittmann, S., Stoiber, T., Berg, A., Ankel-Fuchs, D., and Möllmann, U. (2002) Highly antibacterial active aminoacyl penicillin conjugates with acylated biscatecholate siderophores based on secondary diamino acids and related compounds. *J Med Chem* **45:** 3032–3040.
Hissen, A.H., Wan, A.N., Warwas, M.L., Pinto, L.J., and Moore, M.M. (2005) The *Aspergillus fumigatus* siderophore biosynthetic gene *sidA*, encoding l-ornithine N5-oxygenase, is required for virulence. *Infect Immun* **73:** 5493–5503.
Hof, C., Eisfeld, K., Welzel, K., Antelo, L., Foster, A.J., and Anke, H. (2007) Ferricrocin synthesis in *Magnaporthe grisea* and its role in pathogenicity in rice. *Mol Plant Pathol* **8:** 163–172.
Horbach, R., and Deising, H.B. (2013) The biotrophy – necrotrophy switch in fungal pathogenesis. In *The Mycota – XI. Agricultural Applications*. Kempken, F. (ed.). Berlin, Heidelberg, New York: Springer, pp. 343–360.
Horbach, R., Graf, A., Weihmann, F., Antelo, L., Mathea, S., Liermann, J.C., *et al*. (2009) Sfp-type 4′-phosphopantetheinyl transferase is indispensable for fungal pathogenicity. *Plant Cell* **21:** 3379–3396.
Horbach, R., Navarro-Quesada, A.R., Knogge, W., and Deising, H.B. (2011) When and how to kill a plant cell: infection strategies of plant pathogenic fungi. *J Plant Physiol* **168:** 51–62.
Hortschansky, P., Eisendle, M., Al-Abdallah, Q., Schmidt, A.D., Bergmann, S., Thon, M., *et al*. (2007) Interaction of HapX with the CCAAT-binding complex – a novel mechanism of gene regulation by iron. *EMBO J* **26:** 3157–3168.
Hovmoller, M.S., Yahyaoui, A.H., Milus, E.A., and Justesen, A.F. (2008) Rapid global spread of two aggressive strains of a wheat rust fungus. *Mol Ecol* **17:** 3818–3826.
Jain, R., Valiante, V., Remme, N., Docimo, T., Heinekamp, T., Hertweck, C., *et al*. (2011) The MAP kinase MpkA controls cell wall integrity, oxidative stress response, gliotoxin production and iron adaptation in *Aspergillus fumigatus*. *Mol Microbiol* **82:** 39–53.
Kieu, N.P., Aznar, A., Segond, D., Rigault, M., Simond-Cote, E., Kunz, C., *et al*. (2012) Iron deficiency affects plant defence responses and confers resistance to *Dickeya dadantii* and *Botrytis cinerea*. *Mol Plant Pathol* **13:** 816–827.
Lan, C.-Y., Rodarte, G., Murillo, L.A., Jones, T., Davis, R.W., Dungan, J., *et al*. (2004) Regulatory networks affected by iron availability in *Candida albicans*. *Mol Microbiol* **53:** 1451–1469.
Leach, J., Lang, B.R., and Yoders, O.C. (1982) Methods for selection of mutants and *in vitro* culture of *Cochliobolus heterostrophus*. *J Gen Microbiol* **128:** 1719–1729.
Lee, B.N., Kroken, S., Chou, D.Y., Robbertse, B., Yoder, O.C., and Turgeon, B.G. (2005) Functional analysis of all nonribosomal peptide synthetases in *Cochliobolus heterostrophus* reveals a factor, NPS6, involved in virulence and resistance to oxidative stress. *Eukaryot Cell* **4:** 545–555.
Letendre, E.D., and Gibbons, W.A. (1985) Isolation and purification of canadophore, a siderophore produced by *Helminthosporium carbonum*. *Biochem Biophys Res Commun* **129:** 262–267.
Limpert, E., Godet, F., and Müller, K. (1999) Dispersal of mildews across Europe. *Agric For Meteorol* **97:** 293–308.
Malonek, S., Rojas, M.C., Hedden, P., Gaskin, P., Hopkins, P., and Tudzynski, B. (2004) The NADPH-cytochrome P450 reductase gene from *Gibberella fujikuroi* is essential for gibberellin biosynthesis. *J Biol Chem* **279:** 25075–25084.
Marquez-Fernandez, O., Trigos, A., Ramos-Balderas, J.L., Viniegra-Gonzalez, G., Deising, H.B., and Aguirre, J. (2007) Phosphopantetheinyl transferase CfwA/NpgA is required for *Aspergillus nidulans* secondary metabolism and asexual development. *Eukaryot Cell* **6:** 710–720.
Meda, A.R., Scheuermann, E.B., Prechsl, U.E., Erenoglu, B., Schaaf, G., Hayen, H., *et al*. (2007) Iron acquisition by phytosiderophores contributes to cadmium tolerance. *Plant Physiol* **143:** 1761–1773.
Mei, B., Budde, A.D., and Leong, S.A. (1993) *sid1*, a gene initiating siderophore biosynthesis in *Ustilago maydis*: molecular characterization, regulation by iron, and role in phytopathogenicity. *Proc Natl Acad Sci USA* **90:** 903–907.
Miller, M., Zhu, H., Xu, Y., Wu, C., Walz, A., Vergne, A., *et al*. (2009) Utilization of microbial iron assimilation processes for the development of new antibiotics and inspiration for the design of new anticancer agents. *Biometals* **22:** 61–75.
Mishra, P.K., Baum, M., and Carbon, J. (2011) DNA methylation regulates phenotype-dependent transcriptional activity in *Candida albicans*. *Proc Natl Acad Sci USA* **108:** 11965–11970.
Mootz, H.D., Schwarzer, D., and Marahiel, M.A. (2002) Ways of assembling complex natural products on modular nonribosomal peptide synthetases. *Chembiochem* **3:** 490–504.

Möllmann, U., Heinisch, L., Bauernfeind, A., Kohler, T., and Ankel-Fuchs, D. (2009) Siderophores as drug delivery agents: application of the 'Trojan Horse' strategy. *Biometals* **22:** 615–624.

Neilands, J.B., Konopka, K., Schwyn, B., Coy, M., Francis, R., Paw, B.H., and Bagg, A. (1987) Comparative biochemistry of microbial iron assimilation. In *Iron Transport in Microbes, Plants and Animals*. Winkelmann, G., Winge, D.R., and Neilands, J.B. (eds). Weinheim: VCH, pp. 3–34.

Nicholson, R.L., and Moraes, W.B.C. (1980) Survival of *Colletotrichum graminicola*: importance of the spore matrix. *Phytopathology* **70:** 255–261.

O'Connell, R.J., Thon, M.R., Hacquard, S., Amyotte, S.G., Kleemann, J., Torres, M.F., *et al*. (2012) Lifestyle transitions in plant pathogenic *Colletotrichum* fungi deciphered by genome and transcriptome analyses. *Nat Genet* **44:** 1060–1065.

Oide, S., Moeder, W., Krasnoff, S., Gibson, D., Haas, H., Yoshioka, K., and Turgeon, B.G. (2006) NPS6, encoding a nonribosomal peptide synthetase involved in siderophore-mediated iron metabolism, is a conserved virulence determinant of plant pathogenic ascomycetes. *Plant Cell* **18:** 2836–2853.

Oliveira-Garcia, E., and Deising, H. (2013) Infection structure-specific expression of β-1,3-glucan synthase is essential for pathogenicity of *Colletotrichum graminicola* and evasion of β-glucan-triggered immunity in maize. *Plant Cell* **25:** 2356–2378.

Park, Y.S., Choi, I.D., Kang, C.M., Ham, M.S., Kim, J.H., Kim, T.H., *et al*. (2006) Functional identification of high-affinity iron permeases from *Fusarium graminearum*. *Fungal Genet Biol* **43:** 273–282.

Philpott, C.C. (2006) Iron uptake in fungi: a system for every source. *Biochim Biophys Acta* **7:** 636–645.

Philpott, C.C., and Protchenko, O. (2008) Response to iron deprivation in *Saccharomyces cerevisiae*. *Eukaryot Cell* **7:** 20–27.

Punt, P.J., Oliver, R.P., Dingemanse, M.A., Pouwels, P.H., and Van den Hondel, C.A. (1987) Transformation of *Aspergillus* based on the hygromycin B resistance marker from *Escherichia coli*. *Gene* **56:** 117–124.

Ratledge, C., and Dover, L.G. (2000) Iron metabolism in pathogenic bacteria. *Annu Rev Microbiol* **54:** 881–941.

Raymond, K.N., and Carrano, C.J. (1979) Coordination chemistry and microbial iron transport. *Acc Chem Res* **12:** 183–190.

Roosenberg, J.M., and Miller, M.J. (2000) Total synthesis of the siderophore danoxamine. *J Org Chem* **65:** 4833–4838.

Rzhetsky, A., and Nei, M. (1992) A simple method for estimating and testing minimum evolution trees. *Mol Biol Evol* **9:** 945–967.

Schrettl, M., Bignell, E., Kragl, C., Joechl, C., Rogers, T., Arst, H.N.J., *et al*. (2004) Siderophore biosynthesis but not reductive iron assimilation is essential for *Aspergillus fumigatus* virulence. *J Exp Med* **200:** 1213–1219.

Schrettl, M., Bignell, E., Kragl, C., Sabiha, Y., Loss, O., Eisendle, M., *et al*. (2007) Distinct roles for intra- and extracellular siderophores during *Aspergillus fumigatus* infection. *PLoS Pathog* **3:** 1195–1207.

Singh, R.P., Hodson, D.P., Huerta-Espino, J., Jin, Y., Bhavani, S., Njau, P., *et al*. (2011) The emergence of Ug99 races of the stem rust fungus is a threat to world wheat production. *Annu Rev Phytopathol* **49:** 465–481.

Sundström, K.R. (1964) Studies on the physiology, morphology and serology of Exobasidium. In *Symbolae Botanicae Upsalienses*. Melin, E., and Nannfeldt, J.A. (eds). Uppsala, Sweden: Lundequistska bokhandeln, pp. 1–89.

Tamura, K., Dudley, J., Nei, M., and Kumar, S. (2007) MEGA4: molecular evolutionary genetics analysis (MEGA) software version 4.0. *Mol Biol Evol* **24:** 1596–1599.

Timberlake, W.E. (1980) Developmental gene regulation in *Aspergillus nidulans*. *Dev Biol* **78:** 497–510.

Timberlake, W.E. (1990) Molecular genetics of *Aspergillus* development. *Annu Rev Genet* **24:** 5–36.

Valiante, V., Jain, R., Heinekamp, T., and Brakhage, A.A. (2009) The MpkA MAP kinase module regulates cell wall integrity signaling and pyomelanin formation in *Aspergillus fumigatus*. *Fungal Genet Biol* **46:** 909–918.

Vértesy, L., Aretz, W., Fehlhaber, H.-W., and Kogler, H. (1995) Salmycin A–D, Antibiotika aus *Streptomyces violaceus*, DSM 8286, mit Siderophor-Aminoglycosid-Struktur. *Helv Chim Acta* **78:** 46–60.

Wallner, A., Blatzer, M., Schrettl, M., Sarg, B., Lindner, H., and Haas, H. (2009) Ferricrocin, a siderophore involved in intra- and transcellular iron distribution in *Aspergillus fumigatus*. *Appl Environ Microbiol* **75:** 4194–4196.

Weinberg, E.D. (1978) Iron and infection. *Microbiol Rev* **42:** 45–66.

Weinberg, E.D. (2009) Iron availability and infection. *Biochim Biophys Acta* **7:** 600–605.

Wencewicz, T.A., Möllmann, U., Long, T.E., and Miller, M.J. (2009) Is drug release necessary for antimicrobial activity of siderophore-drug conjugates? Syntheses and biological studies of the naturally occurring salmycin 'Trojan Horse' antibiotics and synthetic desferridanoxamine-antibiotic conjugates. *Biometals* **22:** 633–648.

Werner, S., Sugui, J.A., Steinberg, G., and Deising, H.B. (2007) A chitin synthase with a myosin-like motor domain is essential for hyphal growth, appressorium differentiation, and pathogenicity of the maize anthracnose fungus *Colletotrichum graminicola*. *Mol Plant Microbe Interact* **20:** 1555–1567.

Wiemann, P., Albermann, S., Niehaus, E.M., Studt, L., von Bargen, K., Brock, N.L., *et al*. (2012) The Sfp-type 4′-phosphopantetheinyl transferase Ppt1 of *Fusarium fujikuroi* controls development, secondary metabolism and pathogenicity. *PLoS ONE* **7:** e37519.

Yu, J.H., Hamari, Z., Han, K.H., Seo, J.A., Reyes-Dominguez, Y., and Scazzocchio, C. (2004) Double-joint PCR: a PCR-based molecular tool for gene manipulations in filamentous fungi. *Fungal Genet Biol* **41:** 973–981.

Supporting information

Additional supporting information may be found in the online version of this article at the publisher's web-site.